CLM-R255

CLM-R255

UKAEA

Report

THE DEVELOPMENT OF AUSTENITIC STAINLESS STEELS AS LOW-ACTIVITY STRUCTURAL MATERIALS FOR FUSION REACTORS

A. H. BOTT
F. B. PICKERING
G. J. BUTTERWORTH

CULHAM LABORATORY
Abingdon, Oxon

1985

C.18 Available from H. M. Stationery Office Price £5.00

CLM-R 255

THE DEVELOPMENT OF AUSTENITIC STAINLESS STEELS AS LOW-ACTIVITY STRUCTURAL MATERIALS FOR FUSION REACTORS

A H Bott and F B Pickering
Department of Metallurgy, Sheffield City Polytechnic

and

G J Butterworth
Culham Laboratory, Abingdon, Oxon OX14 3DB
(Euratom/UKAEA Fusion Association)

ABSTRACT

A study based on published information has been performed to examine the feasibility of designing low-activity austenitic stainless steels to replace the conventional steels AISI 316, 320 and 321 and the proprietary steel FV548 for use as first wall and blanket materials in a fusion reactor. The alternative compositions have been chosen subject to the condition that the contact gamma ray dose rate associated with the induced radioactivity does not exceed 2.5×10^{-5} Gyh^{-1} after a decay period of 100 years. This limit should permit relatively safe handling of discarded components for subsequent recycling. The approach adopted in designing the alternative alloys involved the replacement of the high-activity elements that occur in conventional stainless steels with elements exhibiting low residual dose rates, while at the same time retaining the fully austenitic structure and equivalent transformation characteristics and mechanical properties. The major replacements suggested were Ni by Mn-N combinations, Mo by W, Ti and Nb by Ta. The compositions proposed for the low-activity steels were assessed with regard to:

(a) the requisite low level of long term dose rate
(b) the constitution, with respect to the austenite/ferrite ratio
(c) phase stability, in terms of the transformation of austenite to martensite and the precipitation of sigma phases
(d) general cold working and formability
(e) void swelling characteristics
(f) mechanical properties and creep resistance.

In terms of these criteria the alternative alloys are expected to have similar characteristics to those of the established steels they are designed to replace. They are, however, predicted to have higher proof stress values and tensile strengths, largely as a consequence of the increased nitrogen content.

August 1985

ISBN: 0-85311-141-3

CONTENTS

1. INTRODUCTION

In order to exploit the potential environmental advantages of thermonuclear fusion with respect to the generation of radioactive waste, the ability to recycle radiation-damaged structural materials from fusion reactors after relatively short-term storage must be maximised. It is anticipated that the first wall and breeding blanket components will need to be replaced several times during a reactor lifetime and that, as a consequence, there will be a steady output of activated radiation-damaged structural material. This material should therefore consist only of those chemical elements for which the induced radioactivity decays sufficiently rapidly to allow the material to be handled safely after a reasonably short nuclear decay period, such as 100 years, so as to permit the possibility of its reclamation.

Activation and decay calculations have quantified the acceptability of most of the chemical elements in terms of the concentrations permitted in the initial unirradiated material, to ensure that the surface dose rate does not exceed the level that would allow essentially unrestricted handling after a reasonably short nuclear cooling period following its service in a reactor. Application of this criterion results in the elimination, at the levels currently employed, of a number of elements commonly utilised as alloying additions in iron-base alloys, specifically Ni, Ti, Al, Mo, Nb and Zr. Some of these elements are integral components of existing steels, in which their presence is required to obtain particular combinations of material properties. In order to meet the above criterion, however, alternative compositions containing acceptable concentrations of more favourable alloying additions must be proposed.

Both austenitic and ferritic stainless steels are currently being assessed as candidate alloys for the first wall and blanket structures of D-T fusion reactors. The austenitic grades have the advantages of greater formability, more ready weldability, absence of ferromagnetism and resistance to embrittlement. Ferritic steels, on the other hand, are generally more resistant to radiation damage, to thermal fatigue and to corrosion in liquid lithium environments.

The present study considers the prospects for developing low-activity stainless steels as alternatives to the well-established austenitic grades AISI 316, 320 and 321 and Firth-Vickers' FV548. Since it is necessary to extrapolate empirical data from the published literature to predict the properties of the alloys proposed, an attempt has been made to maintain the

compositions close to those of materials for which there is maximum available information.

2. MATERIAL SELECTION FOR FIRST WALL AND BLANKET

The most critical materials problem in fusion reactor technology is probably that of the selection and development of suitable first wall and blanket materials. Such components experience the highest fluxes of energetic neutrons, ions, uncharged particles and γ-rays and are thus subject to the highest rates of transmutation and radiation damage. The first wall and blanket structural material must provide a highly reliable interface between the high pressure coolant and the low pressure plasma chamber, yet must be of sufficiently thin section as to avoid excessive thermal fatigue and neutron absorption. The choice of first wall material will therefore depend on the physical, mechanical, chemical and neutronic properties as well as on the susceptibility to radiation damage and ultimately on the availability and cost. Such criteria for the suitability of the various candidate materials proposed have been discussed in several reviews in the literature for both first wall[1-5] and blanket[6-13] components.

A thermonuclear reactor converts the kinetic energy of 14 MeV neutrons and 3.5 MeV helium ions, released by the fusion of deuterium and tritium, initially into heat and ultimately into usable power. To use this fusion reaction the plasma containing D^+, T^+ and He^{2+} ions at a temperature of the order 10^8 K must be magnetically or otherwise confined to prevent contact with any structural elements of the reactor. Moreover, the energy released in the plasma must be removed efficiently and tritium must be bred to produce a continuous supply of fuel. It is the blanket region of the reactor that must fulfill these two functions, being separated from the plasma only by the first wall.

The main mode of energy transfer from the plasma to the power generating equipment is via the heat deposited in the blanket by 14 MeV neutrons, with a small contribution from the deposition of radiation and particles on the first wall surface and some energy gain from the tritium-breeding reactions. A cooling medium flowing through the blanket removes this heat via heat exchangers to conventional power plant. Whilst possible coolants include water and helium the breeding material is limited to lithium or lithium

compounds. Compatibility with the lithium-based breeder material is an important requirement of structural material for the blanket region.

Neutron-nuclei interactions lead to unavoidable radiation damage of reactor materials. Atoms recoiling from impact with neutrons generate cascades of other atoms displaced from their normal lattice positions, leading to the formation of interstitials, vacancies and subsequently dislocation loops. Furthermore, in the presence of a stabilising gas, the clustering of vacancies can result in severe void swelling. Helium and possibly hydrogen generated by transmutation reactions may provide such stabilisation. In addition the neutron-atom interactions result in the transformation of some stable isotopes into radioactive ones, of a different element in some cases. These transmutations may lead to degradation of the structural integrity and to problems in respect of the replacement, storage and reuse or disposal of first wall and blanket materials on account of the induced radioactivity.

In order to transfer heat into the coolant from the first wall and blanket it is necessary to establish thermal gradients. The nature of these gradients will be complicated by the surface heating of the first wall by electromagnetic radiation, charged particles and neutral atoms and the non-uniform nuclear heating in the blanket. In the constrained structural members these thermal gradients will impose thermal stresses that vary during the burn cycle. It will therefore be necessary to employ not only strong but also fatigue-resistant materials.

Since advanced materials development for fusion will involve the optimisation of so many characteristics an important option may be the utilisation of layered composites. Materials specifications will depend on whether a single material has to satisfy all the requirements or whether more appropriate combinations of materials can be exploited[14,15]. Some design approaches, by employing coatings or claddings, permit the decoupling of structural and surface property requirements, thereby expanding the potential of some materials to be used in applications where they would not otherwise be suitable. Coating-substrate systems that have received attention include plasma-spray deposited ceramic claddings on stainless steels[16,17]. Such coatings might reduce incompatibilities in proposed systems, for example by reducing the corrosive influence of lithium on high-nitrogen austenitic stainless steels in a manner analogous to the corrosion-erosion protection of

turbine blades by plasma-sprayed ceramic coatings[16].

Investigations of the influence of lithium exposure on austenitic stainless steels[18-21] include some observations indicating that, beyond the presence of a thin corrosion layer, no matrix grain boundary attack ensues from the exposure of Cr-Mn steel to liquid lithium for 1500 h at 873 K[18]. Moreover, the changes in tensile properties[20,21] under these conditions are largely attributable to the precipitation of carbides different from those formed during ageing in the absence of lithium. The beneficial effect of traces of LiH on the corrosion behaviour of austenitic stainless steels in lithium environments has also been reported[19,20].

In recent years much effort has been devoted to materials research associated with the development of prototype and first-generation fusion reactors[22-26]. Conceptual studies of commercial fusion power systems have raised the issues of occupational and public health and safety, particularly with regard to the recycling or disposal of activated structural waste material. The waste management aspect of fusion power systems has been examined in a number of recent studies[13,27-35] and quantified to the extent that permitted concentrations have been specified for most of the chemical elements that may be present in first wall and blanket materials, in order that end-of-service components will meet particular guidelines for recyling or permanent disposal[36]. Furthermore, analogies between fission and fusion wastes, together with a consideration of current nuclear waste disposal regulations, have provided a basis upon which 'waste disposal ratings' have been calculated for a number of candidate reactor materials[37]. Thus sufficient quantitative data are available to permit the elemental tailoring of alloy compositions to yield potential low-activity candidate materials, the probable properties of which may then be semi-quantitatively predicted by extrapolation of experimentally-derived relationships available in the literature.

3. THE CONSTITUTION OF STAINLESS STEELS

Many workers have investigated the constitution of a wide range of Fe-Ni-Cr alloys and its extension into more complex alloys of the types currently available as standard grades of stainless steel[38-45]. The compositional

range over which the single austenitic γ phase remains stable in Fe-Ni-Cr alloys contracts with decreasing temperature, the α ferrite, δ ferrite (a high temperature allotropic form of α) and σ (an intermetallic compound based on FeCr) phases remaining more stable at lower Cr contents. The addition of increasing amounts of Ni to 18% Cr steels enlarges the γ-loop in the pseudobinary equilibrium phase diagram, resulting in two major constitutional effects:

(1) the amount of the austenite (γ) phase present at the solution temperatures is increased

(2) the M_s temperature of that austenite, at which it transforms to metastable body-centred cubic martensite, is lowered such that at and above about 8% Ni the austenite remains stable on cooling from the solution treatment temperature to room temperature[42,43,45,46]. In commercial stainless steels, however, the influence on the constitution exerted by the other alloying elements present is often critical. These other elements will increase or decrease the austenite stability, depending on whether they are austenite or ferrite stabilisers. In much of the published work the correlation between alloy composition and constitution (following rapid cooling from high solution treatment temperatures) has been assessed through the calculation of chromium and nickel equivalent compositions with respect to the elements present in the material. These equivalents have then been applied by reference to Schaeffler-type[47-49] diagrams to the constitution of commercial alloys.

It must be borne in mind that the amounts of some elements remaining in solid solution may be altered by precipitation phenomena in those alloys containing carbides and carbonitrides. The extent of such carbide-carbonitride precipitation in a solution treated alloy can, however, be estimated from experimentally-derived solubility relationships available in the literature for the commonly observed carbides in commercially relevant stainless steels, for example for NbC in austenite[51,52]. Whilst such an approach can indicate the potential for precipitation of particular carbides or nitrides, both the extent of the precipitation and the composition of the phases precipitated can be influenced by kinetic considerations. For instance, despite the fact that NbC and TiC are thermodynamically the most stable

carbides in austenitic stainless steels, thermal exposure of solution treated steels at temperatures in the range 550^0–700^0C can result in the preferential precipitation of $M_{23}C_6$ before NbC/TiC[50,53,54].

Standard austenitic stainless steels contain a range of chromium and nickel contents and some grades, for example AISI 321, 347 and FV548, are stabilised against $Cr_{23}C_6$ precipitation by additions of Ti and Nb. It is quite common to increase the nickel content to compensate for the ferrite-forming tendency of Ti and Nb and also for the removal from solid solution of the austenite-forming interstitials C and N as stable carbonitrides. In contrast, austenitic stainless steels with lower nickel contents have been developed by exploiting the austenite-forming propensities of manganese and nitrogen, in combination with slightly higher carbon levels. Such alloys, for example the AISI series 200 steels, typically contain 3-6% Ni, 5-10% Mn and about 0.25% N, as compared with up to 22% Ni (AISI 310) in the 300 series alloys.

The carbon and nitrogen contents can each be increased to as much as 0.8% but are usually limited to less than 0.4%[46,55-58]. The use of nitrogen at concentrations as high as 0.4% necessitates the replacement of some Ni by Mn in order to guarantee sufficient nitrogen solubility to avoid porosity problems during solidification. Nickel is commonly regarded as decreasing the solubility of N whereas Mn and Cr allow more to be retained in solution[46]. Even more extensive use of Mn or Mn and N to replace Ni has been made in some commercial alloys, eg Tenelon, Nonmagne, NM-1, 25-5-1, 31-7 and JUS289N[37].

4. PHASE STABILITY

In the case of the less highly alloyed austenitic stainless steels a transformation of at least part of the austenite to martensite occurs. For alloys in which the M_s temperature is above room temperature this transformation can occur on cooling from solution treatment temperatures. Where the austenite phase is more stable the martensite transformation may only be induced by refrigeration. Even in these more stable alloys, however, the M_d temperature at which deformation induces the formation of martensite may still be above room temperature; hence martensite may be formed during deformation. This effect has an important bearing on the formability of

components. It is generally accepted that the M_s temperature is depressed by almost all alloying elements, except Co[59-61]. Predictive equations which relate M_s to the composition have been determined specifically for austenitic stainless steels.

Another consequence of microstructural instability in austenitic stainless steel is the tendency to form intermetallic phases. The complexity of composition of commercial alloys leads to a variety of possible intermetallic phases. Topographically close-packed phases, even in quite small volume fractions, are generally detrimental to low and high temperature properties, including the ductility, toughness, strength and creep ductility. Their presence can provide easy paths for fracture and can deplete both the grain boundary and matrix of important solid solution strengthening elements. The principal types of intermetallic compound occurring in stainless steels include[62] sigma phase, chi phase and Laves phase, of which sigma is by far the most important since it is an equilibrium phase in the Fe-Ni-Cr system and has a wide compositional range. It is generally referred to as FeCr though it can be FeMo and can, moreover, dissolve appreciable quantities of other elements.

Sigma phase is generally formed in austenitic stainless steels on heating at 700^0-950^0C, this tendency being accentuated by increasing Cr content and the presence of elements such as Mo, Ti and Si[46]. Sigma phase has been found to precipitate very slowly from a fully austenitic structure though if delta ferrite is present the transformations are considerably accelerated[63]; this occurs because delta ferrite is richer in Cr than the austenite and because diffusion is more rapid in the bcc delta ferrite. All ferrite-forming elements partition to the delta ferrite and many of them promote sigma formation[64,65]. The effect of $M_{23}C_6$ particles on the kinetics of sigma phase nucleation has received some attention though there is no general agreement as to exactly how this carbide influences sigma formation[66-70].

The propensity for sigma phase formation in stainless steels and superalloys has been much investigated and one particularly successful approach involves an evaluation of the electron vacancy number. It has been found that the average number of unpaired electrons in a metallic system can be related to the tendency to form electron-compounds, of which the sigma phase is one. In

as early as 1938 a publication appeared in which theoretical and experimental results were combined to provide a coherent explanation of the valence electron behaviour of Cr, Mn, Fe, Co and Ni[71]. It was postulated that the higher the number of unpaired electrons the greater would be the ability of an element to form electron compounds. Later work modified the early results to facilitate their application to alloys[72-75], characterising the range of composition over which sigma phase would form by an average electron vacancy number, N_v, of the solid solution matrix. Subsequent refinements[76-79] have permitted successful application of the predictive equations to commercial alloys.

Precipitation effects of the kind just described are likely to be important in affecting the properties of reactor components during service.

5. VOID SWELLING

Void swelling in irradiated materials was experimentally observed in austenitic steels in the mid-1960's[80,81], more than five years after its prediction[82]. In these materials void formation can induce volumetric swelling of over 20% and lead to severe engineering problems in highly-irradiated reactor components. Essentially, void swelling occurs through a supersaturation of vacancies and interstitials resulting from atomic displacement cascades[83]. Dislocations have a slightly higher preference for the capture of interstitials and the excess vacancies which result migrate to form clusters that are stabilised by residual gases inherent in the steel or generated by transmutations.

It is well established that austenitic alloys exhibit a wide range of void-swelling behaviour[83-87] depending on the irradiation conditions, temperature, composition and degree of cold work. The influence of composition and constitution on void swelling behaviour has been examined both for pure Fe-Ni-Cr alloys and commercial stainless steels[83,88-90]. For austenitic steels at temperatures in the range 400^0C-600^0C swelling is a maximum when the composition lies in a three-phase field, a minimum when it lies in the single-phase austenitic field and has an intermediate value in two-phase regions[91]. It is possible to correlate void swelling with the electron vacancy concentration and stacking fault energy of the

matrix[79,91]. It has been suggested that below a critical value of N_v negligible void swelling will occur, whilst above this value the swelling will increase with higher N_v. This proposition is probably based on the fact that these critical N_v values correspond to compositions at which structural transformations take place. If this is the case, especially where sigma formation is involved, the kinetics of such transformations will be critical.

6. FABRICATION AND MECHANICAL PROPERTIES OF AUSTENITIC STAINLESS STEELS

6.1 Deformation-induced martensite transformation

In austenitic stainless steels, even when the chosen composition ensures that the M_s temperature is below room temperature, the M_d temperature may still be above room temperature and thus martensite may be formed during deformation at any temperature below M_d. Whilst two martensitic phases, α'- martensite (with body centred cubic/body centred tetragonal structure) and ε- martensite (hexagonal close-packed) have been identified in austenitic steels, the main emphasis of predictive equations to be found in the literature has been placed on the prediction of the M_d temperature for α' formation and its relationship to M_s[46,59,61,92-94]. Whilst an excessive instability of the austenite would be undesirable, a critical amount of deformation-induced martensite has been shown to be essential for good stretch formability[46].

6.2 Stacking fault energy

The work hardening rate exhibited by austenite during fabrication will depend on its stacking fault energy, a lowering of the stacking fault energy having the effect of increasing the work hardening rate[95]. The stacking fault energy (SFE) will, in turn, depend on the composition of the austenite solid solution, being decreased by such elements as Cr, Mo, Co, Si, C and N[96-98] and increased by Ni and Cu[96,99]. The application of linear regression techniques to experimental results has provided some degree of quantification of these effects in the form of predictive relationships between SFE and composition for several alloying elements in solution in the austenite[100,101].

6.3 Structure-property relationships

The AISI 300 series of austenitic stainless steels, free from delta ferrite and stable with respect to martensite formation, have low proof stress values in the region of 250 MPa in the solution treated condition. Much higher values of proof stress and tensile strength have been achieved through the increasing replacement of Ni by combinations of Mn, C and N, as in the 200 series alloys and to an even greater extent in the Tenelon-type materials, in which strength increases of up to 300% have been attained. The interstitial solutes are the most effective solid solution strengtheners and nitrogen is very potent in this respect. Excellent correlations have been obtained between compositional and microstructural parameters and the tensile strength and proof stress values of austenitic stainless steels, a thorough appraisal of which has been presented in the literature[46,102-104].

6.4 Formability

In commercial applications the fabrication of stainless steel components frequently involves cold working by either deep drawing or stretch forming. For the latter in particular a high maximum uniform strain is essential. In a steel that retains a totally austenitic structure on deformation at ambient temperature the work hardening rate decreases continuously as the strain increases. The value of the work hardening rate relative to the flow stress will be crucial to the stretch formability since the maximum uniform strain occurs when these two parameters are numerically equal.

In cases where the steel composition results in a less stable austenite, the presence of any deformation-induced martensite will cause the flow stress to increase rapidly as the martensite itself begins to participate in the deformation. The overall result is an increase in the work hardening rate to a level above that for a stable steel at the same strain. This relative instability of the austenite can be beneficial to the stretch forming properties since, although the initial work hardening rate will be low, it will increase rapidly at intermediate strain levels to a maximum as more martensite is formed and subsequently decrease as the formation of strain-induced martensite ceases[46]. It is therefore most important that the strain-induced martensite transformation occurs at the appropriate stage of the deformation in order to obtain the highest value of the maximum

uniform strain and hence the optimum stretch formability[46,103,105].

7. ELEMENT ACCEPTABILITY

The relationship between the elemental composition of a first wall or blanket material and the potential for its reclamation or disposal after service in a reactor has been examined by Jarvis[36]. Since it will probably be increasingly important in the future to conserve material resources and to minimise discharges of radio-active waste to the environment, there is a strong incentive to develop schemes for the recycling rather than the permanent disposal of activated structural wastes. As one scenario, the possibility has been considered of reprocessing discarded material and refabricating it into new reactor components by normal methods, following an appropriate period of storage to allow most of the activity to decay. Since protection from direct α and β particle emissions is relatively easily provided, the ability to reprocess material with unrestricted access will mainly depend on the γ dose rate that would be experienced by a worker in contact with the material. Thus it is reasonable to assume that material could not be reworked until the surface dose rate from a large volume of the material has fallen below the level of 2.5×10^{-5} Gyh^{-1}, which represents the current maximum permissible dose rate to an operator working for a 40h week. In calculating the dose rate it is necessary to include the contribution due to the bremsstrahlung from β particles.

On the basis of the above dose rate criterion and an assumed nuclear decay time of 100 years the maximum permissible concentrations in a first wall material of most of the stable elements are indicated in Table 1, taken from Ref 36. The concentrations tabulated here refer to the permitted mass of a particular element relative to the mass that the first wall would have if it consisted solely of that element. It is therefore necessary to make adjustments for the differing densities of the elements when calculating their allowed concentrations in a particular alloy.

Of the major alloying elements employed in austenitic stainless steels, Table 1 shows that iron and chromium may be used in unlimited concentrations. Nickel, however, is permitted only at concentrations below 1%. Molybdenum, often present at a concentration around 2% in conventional steels, must be kept below 0.02%, while niobium can be tolerated only at the extremely low

Table 1 Summary of element acceptability in structural materials from considerations of recycling after 100 years decay time

A. Structural elements (Intended constituents)	
Primary constituents:	C, Mg, V, Cr, Mn, Fe, Ta, W
Major constituents (10-50%):	Si
Minor constituents (1-10%):	Cu, Zn
Trace constitutents (0.1-1%):	Ti, Co, Ni
Undesirable constituents (10-1000 ppm):	Al, Zr, Mo, Sn
Troublesome constituents (1-10 ppm):	Nb
B. Impurity elements	
Unlimited (> 10%):	Li, Be, B, N, O, F, Na, P, S, Ga, Ge, As, Se, Br, Y, Rh, Pd, Sb, Te, I, Cs, Ce, Pr, Nd, Sm, Ho, Yb, Lu, Hf, Os, Au, Hg, Tl, Pb
Minor impurities (1-10%):	Ru, In
Trace impurities (0.1-1%):	Cl, Rb, La, Gd, Pt
Acceptable impurities (10-1000 ppm):	Ca, Sc, Sr, Cd, Dy, Er, Tm, Re
Troublesome impurities (1-10 ppm):	K, Ba
Unacceptable impurities (< 1 ppm):	Ag, Eu, Tb, Ir, Bi, Th, U
C. Omissions	
Hydrogen:	H, D
Unstable elements:	Tc, Pm
Inert gases:	He, Ne, Ar, Kr, Xe

level of 2 ppm. The fact that manganese, tungsten and tantalum are favoured elements suggested the desirability of replacing nickel by some combination of manganese and nitrogen, of molybdenum by tungsten and of niobium and titanium by tantalum. These potential substitution elements are selected because information on their effects in austenitic steels is available for extrapolation.

It will also be noted from Table 1 that elements classed as 'unacceptable impurities', including silver, europium, bismuth and uranium, affect the long term dose rate even when present at concentrations below 1 ppm. Future assessment of the potential of low-activation alloys will therefore need to take into account the likely impurity content of the starting materials.

8. DESIGN OF LOW-ACTIVITY ALLOYS

The standard austenitic stainless steel types 316, 320, 321 and FV548 have been relatively well investigated and, in view of the established position held by these materials, it was decided to base the alternative low-activity alloys on the compositions listed in Table 2. As discussed in the preceding section the unacceptable elements in the conventional steels are Ni, Mo, Ti and Nb, with permitted levels of only 0.1, 0.2, 0.2 and 0.0002 mass % respectively. Possible substitutes for the above elements would be:

(1) Ni by Mn-C-N combinations
(2) Mo by W
(3) Ti and Nb by Ta or Hf.

8.1 Constitution

The constitution of austenitic steels at ambient temperature following rapid cooling from high solution treatment temperatures can be predicted by means of a Schaeffler-type diagram in conjunction with calculated nickel and chromium equivalent values for the principal alloying and impurity elements. Whilst various values have been derived for these chromium and nickel equivalent coefficients, the following relationships have been successfully applied to a wide range of austenitic steels[46,49,50]:

Table 2 Steel Compositions

(a) standard austenitic stainless steels

Element	Steel composition in mass percent			
	316	320	321	FV548
C	0.03-0.06	0.06 max	0.08 max	0.06-0.09
N	0.02 max	0.02 max	0.02 max	-
Ni	10-14	10-14	9-12	11-12
Cr	16-18	16-19	17-19	16-17
Mn	2 max	2 max	2 max	2 max
Si	1 max	1 max	1 max	0.6 max
Mo	2-3	2-3	-	1.0-1.75
Nb	-	-	-	1.05 max
Ti	-	0.3 min	0.4 min	0.005 max
B	-	-	-	0.001-0.003

(b) replacement alloys

Element	Steel composition in mass percent					
	HNA1	HNA2	316T	320T	321T	FV548T
C	0.08 max	0.08 max	0.03-0.06	0.06 max	0.08 max	0.06-0.09
N	0.22-0.36	0.22-0.36	0.23-0.36	0.20-0.36	0.20-0.36	0.26-0.36
Cr	16-18	14-16	16-18	16-19	17-19	16-17
Mn	10-12	10-12	10-14.5	10-14.5	8-11.5	12
Si	1.0 max	1.0 max	1.0 max	1.0 max	1.0 max	0.6 max
W	2-3	1.5-2.5	4-6	4-6	0.7-1.1	2-3.5
Ta	1.5	1.5	0.84-1.68	1.68 max	2.4 max	1.68-2.71

$$\text{Cr equivalent} = (Cr) + 2(Si) + 1.5(Mo) + 5(V) + 5.5(A\ell) + 1.75(Nb) + 1.5(Ti) + 0.75(W)$$

$$\text{Ni equivalent} = (Ni) + (Co) + 0.5(Mn) + 0.3(Cu) + 30(C) + 25(N)$$

where ( ) = mass percent of the element in solution.

Application of the above equations must take account of the removal of any species from solution by, for example, precipitation of carbides or carbonitrides.

Since the concentration of Ti in the alloys is limited by activation considerations it is proposed that Ta should be employed as a substitute. Tantalum is chosen in preference to Hf on the grounds that the extrapolation of existing carbide solubility data for NbC to the tantalum carbides present in the low-activity alloys will be less uncertain, since there is a closer similarity between TaC and NbC than between HfC and NbC, with respect to the heats of formation and crystal structures[106].

Of several empirical solubility relationships for NbC in austenite the following two are the most pertinent[50,51]:

$$\log[Nb][C] = -\frac{9350}{T} + 4.55 \qquad (1)$$

$$\log[Nb][C] = -\frac{8358}{T} + 4.07 \qquad (2)$$

where [ ] = mass percent in solid solution
T = absolute temperature.

Equation 1 was obtained for an 18Cr-13Ni-Nb steel and Eq.2 for a 20Cr-25Ni-Nb steel. If the above relationships are used to estimate the extent of Ta (C,N) solution at anticipated first wall or blanket temperatures of 500°C-600°C then 32-69ppm Ta and 2-5ppm (C+N) would be expected to be dissolved in the austenite.

It is clear that increasing Ni levels may raise the solubility of NbC in austenite and there will probably be a similar effect with TaC. This effect

is opposite to that generally accepted as applicable to the solubility of $M_{23}C_6$ in austenite. Also, there are grounds to expect that increased Mn levels may have the same effect on the solubility of TaC in austenite and, indeed, Mn is known to increase the solubility of nitrides in low alloy steels. A further factor must be considered, however, namely the potential for $M_{23}C_6$ precipitation. At the expected operating temperatures the composition of a precipitating phase may be dictated by kinetic rather than thermodynamic considerations. For example, despite the fact that TaC would be more stable thermodynamically than $M_{23}C_6$, the latter will form more rapidly on account of the kinetics, as it does relative to NbC or TiC in stabilised stainless steels at elevated temperatures. Such $Cr_{23}C_6$ precipitation could pose problems both from the loss of corrosion resistance by localised removal of Cr from solid solution and from the potential loss of ductility by the cellular precipitation at grain boundaries that is observed for chromium carbides and nitrides at some C:N ratios. Any 'excess' carbon remaining in solid solution and acting as an austenite stabiliser would increase the risk of these problems. The potential benefits of the proposed alloys in this respect would therefore be maximised by the precipitation of all carbon in combination with Ta prior to service, with the emphasis on Mn and N contents to stabilise the austenite. Thus, assuming carbon and a similar amount of N to be precipitated from solid solution in combination with Ta, calculations can be performed to compare the likely constitution and properties of the proposed low-activity compositions with standard grades of austenitic stainless steels, the compositions of which are listed in Table 2.

8.1.1 Replacement of manganese by nitrogen

In view of the potential problems that would ensue from the volatilisation of Mn at the operating temperatures and in the high vacuum environment of the first wall or blanket, it seems prudent to attempt to replace it by other austenite stabilisers. One option is nitrogen, others being carbon and copper. There are drawbacks associated with an increased carbon content, in particular carbide precipitation, reduced corrosion resistance and embrittlement, whilst copper would be of limited value since its rather high induced activity restricts its allowable concentration to less than 1%. The most promising modification to the initial alloy composition therefore appears to be an increase in the nitrogen level. By comparing the nickel

equivalent coefficients, namely 0.5 for Mn and 25 for N, it is seen that a manganese concentration of 10-12% should suffice if the dissolved nitrogen content is raised to 0.2-0.35% (Table 2). Such nitrogen levels are quite common in some of the higher strength austenitic stainless steels and also in the nickel-replacement steels of the AISI 200 type. These modifications led to the proposed HNA1 (high nitrogen alloy) composition and subsequently to HNA2, on the basis of which it was considered that similar high nitrogen replacement low-activity compositions should be proposed for AISI 316, 320, 321 and FV548 grades. The suggested compositions are given in Table 2.

The constitutions and potential ranges of properties for the replacement alloys will now be examined. The analysis ranges quoted in the replacement alloy specifications are designed to reflect, as far as practicable, those of the standard counterparts, while fulfilling both the criteria outlined earlier concerning the relative amounts of C, N and Ta and the need to maintain acceptably high levels of austenite stability using N rather than Mn. It is the subsequent application of predictive equations to the composition ranges that leads to the property ranges presented for each alloy, as will be discussed later.

8.1.2 Phase stability

Table 3 lists the Cr and Ni equivalents for the alloys under consideration. These values enable the stability of the resulting austenite to be assessed with reference to Figs.1 and 2[49,50]. The elementally-tailored alloys 316T, 320T, 321T and FV548T replacing the corresponding conventional grades were designed to coincide with the latter on the Schaeffler diagrams, having been selected to have Cr and Ni equivalent characteristics identical to those of the standard steels they replace. The rectangles in Figs.1 and 2 indicate the limits corresponding to the composition ranges for the replacement alloys, in accordance with Table 2b. From Figs.1 and 2 it can be seen that the structure for alloy HNA2 should be 100% austenite for the mid-specification range Cr equivalent value and above mid-specification Ni equivalent value. Such would be the case, however, only for HNA1 and the other replacement alloys in which the Cr equivalent was below mid-specification and the Ni equivalent was above mid-specification. Thus the alloy HNA2 is rather more tolerant to compositional variation than the other replacement alloys. A further assessment of austenite stability may be made

Table 3 Chromium and nickel equivalent values

Alloy	Chromium equivalent	nickel equivalent
316 316T	19.0-24.5	10-15
320 320T	19.0-25.5	10-15
321 321T	17.5-21.8	9-13
FV548 FV548T	17.5-21.7	11-13
HNA1	17.5-22.5	10-14
HNA2	15.1-20.1	10-14

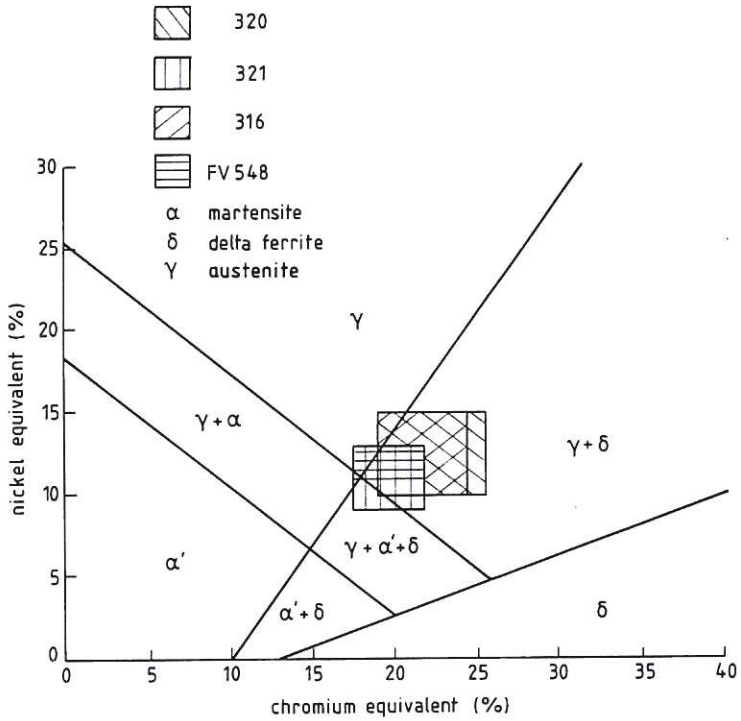

Fig. 1 Schaeffler diagram showing the regions representing the conventional and equivalent replacement austenitic stainless steels.

CLMR255

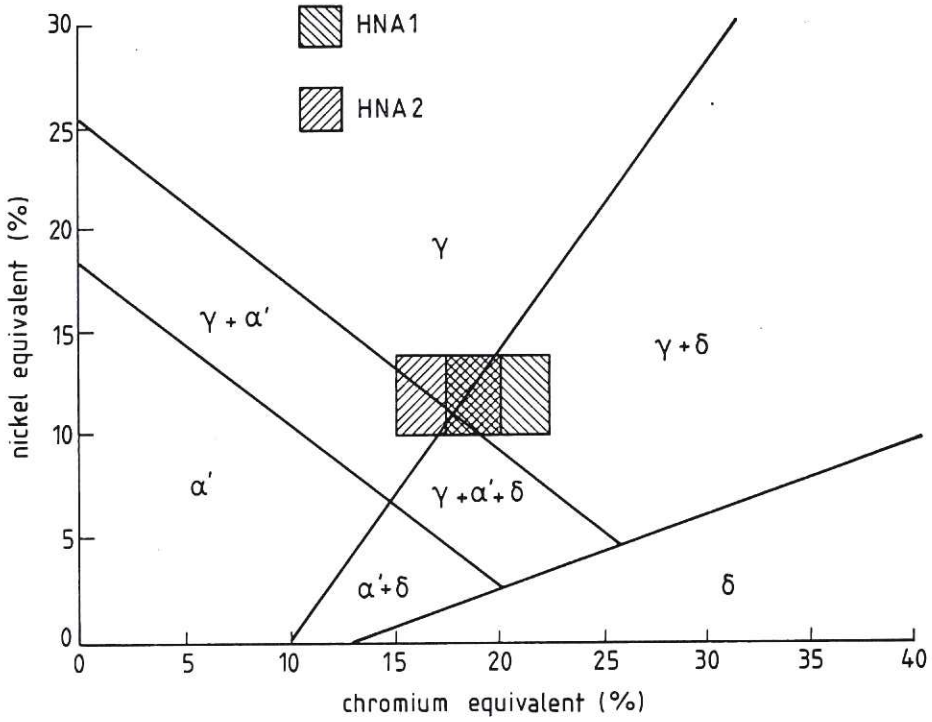

Fig. 2 Schaeffler diagram showing the regions representing the high-nitrogen alloys HNA1 and HNA2.

CLMR255

on the basis of the potential to form martensite at sub-zero temperatures or on cold forming. The following relationships between M_s and M_f temperatures and composition have been used[46], M_f being the temperature at which transformation to martensite is complete:

M_s (^{0}C) = 502 - 810(C) - 1230(N) - 13(Mn) - 30(Ni) - 12(Cr) - 54(Cu) - 46(Mo)

and $M_f \simeq M_s - 140^0$C

The results of calculations using the above equations are presented in Table 4 and compared for the various alloys in Fig.3. Several of the calculated M_f temperatures are unattainable, being below absolute zero, but are included in the diagram merely for comparison. It can be seen that the behaviour of all the proposed replacement alloys compares well with that of their conventional counterparts and, in the case of 321T, the stability with respect to martensite formation is superior to that of the conventional steel.

Studies of some high-Mn austenitic stainless steels have revealed that there may be a risk of a surface martensite transformation due to diffusional loss or evaporation from the surface or internal segregation to precipitates of specific elements that normally stabilise the austenite, eg Ni, Mn, Cu, C, N[11]. In an 8% Mn, 7.2% Ni, 0.19% N, 19% Cr alloy (ICL 016) this effect was found to be restricted to a surface layer 40 μm thick after annealing for 65h at 700^{0}C and cooling to room temperature. In other work[107] on a 17.5% Mn, 0.67% Ni, 0.057% N, 10% Cr alloy it was observed that a similar surface phase instability occurred only for annealing temperatures above 500^{0}C and then only under HVEM irradiation. It was, moreover, conceded in this case that the phenomenon was probably a thin foil effect.

It should be noted that both α' and ε martensites are metastable phases that revert to austenite at higher temperatures[94] and it appears to be generally accepted that α' reversion is complete by about 400^{0}C, though no such unanimity exists regarding ε reversion. There are indications that during rapid heating in some austenitic alloys ε reversion starts at about 500^{0}C and is complete by 600^{0}C. These temperatures have been reported to be reduced to 400^{0}C and 500^{0}C, respectively, under irradiation[108]. If this is the case

Table 4 Martensite transformation susceptibility

Alloy	M_s (^{0}C)		M_f (^{0}C)	
	max	min	max	min
316	-82	-298	-222	-438
320	-82	-310	-222	-450
321	+28	-112	-112	-252
FV548	-66	-139	-206	-270
HNA2	-42	-265	-182	-405
316T	-66	-284	-206	-424
320T	-66	-296	-206	-436
321T	-52	-232	-192	-372
FV548T	-92	-202	-182	-405

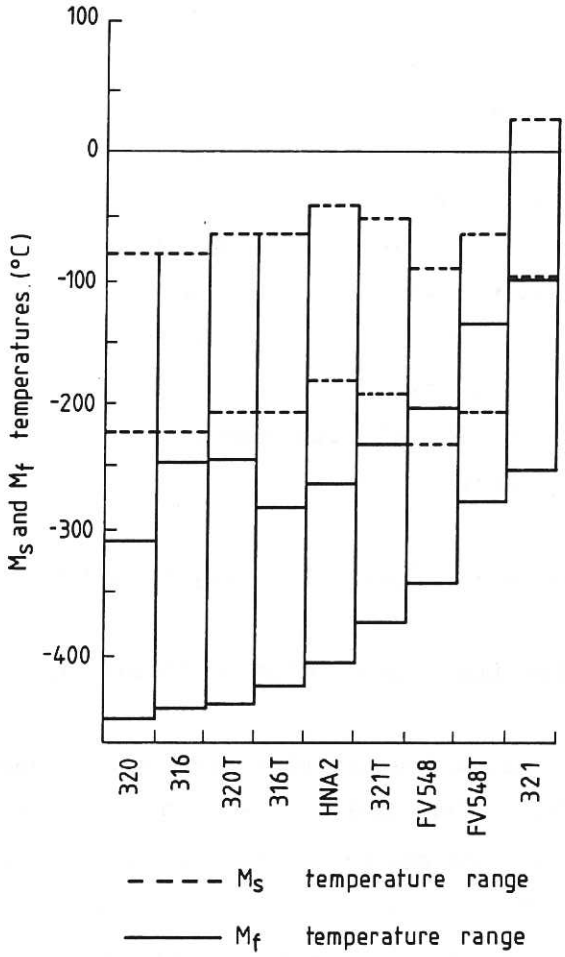

Fig. 3 Chart showing the susceptibility to martensite transformation. The ranges indicated correspond to the upper and lower limits of the composition ranges listed in Table 2.

CLMR255

then the proposed replacement alloys, should they be susceptible to such an instability, would still be fully austenitic at operating temperatures above 500^0C.

Another aspect of the constitution also needs to be examined, namely the potential to form the sigma phase. One approach involves the calculation of N_v values (electron vacancy numbers), which relate the mean number of unpaired electrons in an alloy to the tendency to form electron compounds, one of which is the sigma phase. It is generally found that alloys for which $N_v \geq 2.5$ are prone to sigma formation whilst those with $N_v < 2.5$ are not[72]. These values are not universally accepted, however; some workers placing the sigma threshold at $N_v = 2.95$. It is often possible to characterise the range of composition over which sigma phase would form by an average electron vacancy number of the solid solution matrix, which can be represented by a linear combination of terms:

$$N_v = 4.66(Cr+Mo) + 3.66(Mn) + 2.66(Fe) + 1.71(Co) + 0.61(Ni)$$

where ( ) = atom fraction of element in solution.

More recent work[79] has suggested that some of the above coefficents should be revised to 3.4(Cr), 3.5(Fe) and 2.9(Ni). Table 5 indicates the results of calculations based on the above relationships and the values of N_v for the present alloys are compared in Figs.4 and 5. The predicted resistance to sigma formation varies considerably, according to whether it is based on the modifications proposed by Cawley[79] and derived from experimental work on austenitic stainless steels, or on the more theoretically-founded relationship proposed by Rideout[72], which is perhaps more applicable to the nickel-based superalloys. The Rideout values indicate that all of the replacement alloys would exhibit a stronger tendency towards sigma formation than would the conventional grades, whereas the Cawley values predict that alloy HNA2 would be better than the standard alloys in this respect. In both cases, however, all N_v values lie above the 2.5 'threshold', though in practice the thermodynamic tendency to form the sigma phase will not be the sole factor. In fact, because of the relatively short service life anticipated for first wall materials, the kinetics of sigma generation may well be decisive in determining the acceptability of an alloy.

Table 5 Calculated electron vacancy number (N_V) values

Alloy	Electron vacancy number, N_V	
	after Rideout[72]	after Cawley[79]
316	2.86-2.87	3.45-3.48
320	2.83-2.84	3.39-3.45
321	2.81-2.83	3.36-3.41
FV548	2.81-2.82	3.13-3.15
HNA1	3.18-3.22	3.54-3.58
HNA2	3.10-3.12	3.05-3.10
316T	3.33-3.50	3.67-3.70
320T	3.33-3.57	3.67-3.84
321T	3.14-3.19	3.52-3.50
FV548T	3.24-3.33	3.62-3.68

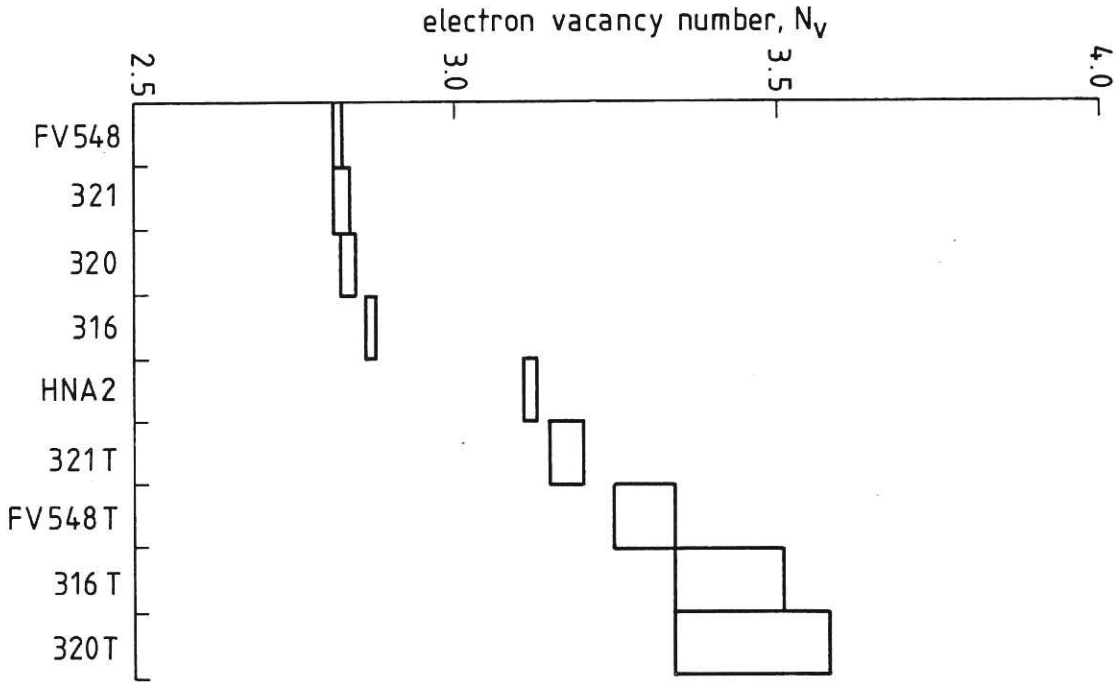

Fig. 4 Electron vacancy numbers for the alloys according to the relationship of Rideout[72]. The ranges indicated correspond to the composition limits given in Table 2.

CLMR255

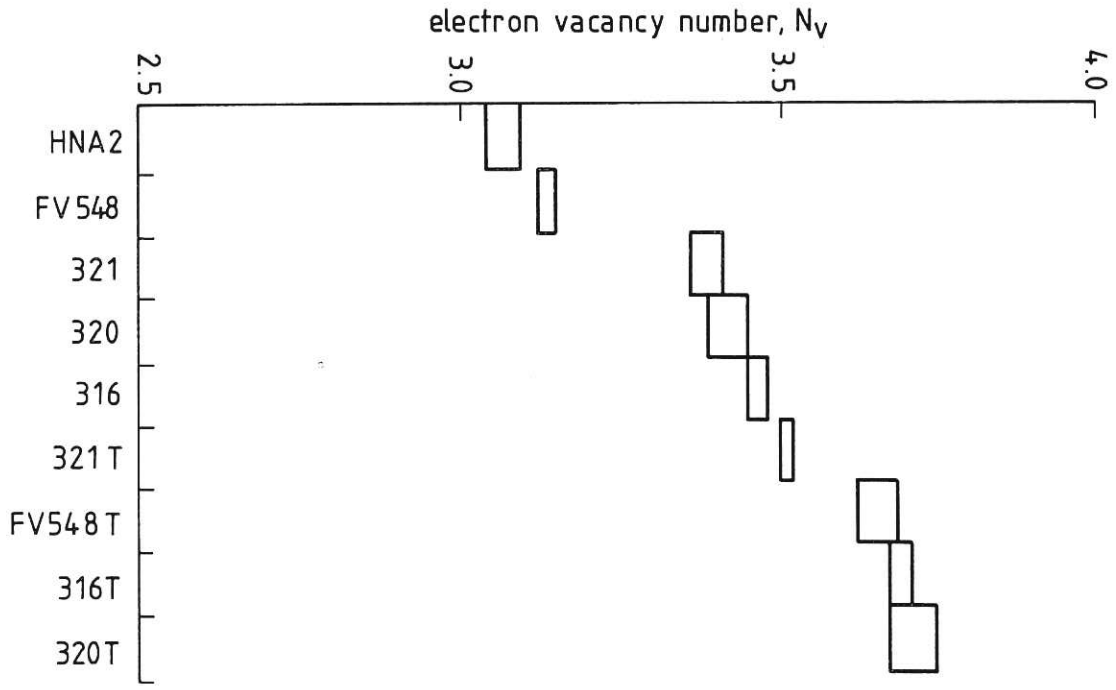

Fig. 5 Electron vacancy numbers for the alloys according to the relationship of Cawley[79]. The ranges correspond to the composition limits given in Table 2.

CLMR255

The kinetics of sigma-phase formation are difficult to predict in the absence of experimental data for alloys having the Mn and N concentrations suggested for the potential replacement materials. Studies of transformations in a duplex γ/δ stainless steel, however, have provided kinetic data indicating that at operating temperatures around 500^0C sigma phase would start to form only after about 10,000h [63], as illustrated by Fig.6. In the case of the proposed alloys the nucleation period would probably be considerably longer, in the absence of both delta ferrite and Cr-rich $M_{23}C_6$, both of which have been found to accelerate the nucleation rate of sigma phase. Furthermore, studies of the behaviour of 316 stainless steel fuel cladding, irradiated in the Dounreay fast reactor at temperatures up to 700^0C, showed no evidence of sigma phase even though this would have been expected under similar conditions in the absence of radiation[79].

8.1.3 Void swelling

The void swelling characteristics of Fe-Ni-Cr alloys and commercial austenitic steels have been correlated with the electron vacancy concentration of the matrix[50,79]. Figure 7 illustrates a rapid increase in the volume swelling generated in commercial steels by irradiation to 40 dpa at 600^0C-625^0C with 46.5 MeV Ni^{6+} ions, for N_v values above 2.5. This increase has been attributed to the onset of structural changes, eg. sigma formation, though this interpretation would be contrary to the effects of sigma 'suppression' in the 316 material mentioned above. If the above work is used as a basis for prediction of the volumetric swelling of the proposed low-activity compositions then, for the above irradiation conditions, extrapolation would give a value in excess of 6%.

Void formation has also been studied in some steels in which Ni has been partially replaced by Mn, N or Cu. In one investigation[109] on the commercial austenitic steel ICL 016, containing 8% Mn, 0.19% N, 19% Cr and 7.2% Ni, swelling ranging from 1.8% to 7% was observed for, respectively, solution treated material without implanted helium and solution treated and aged material containing 10 appm He. Both materials were irradiated to 60 dpa at 625^0C with 46.5 MeV Ni^{6+} ions. The effect was considered to be an average type of swelling response though the reduction in swelling resulting from pre-ageing at 700^0C was noted, as was the potential for further improvement by cold working. It was noted, moreover, that voids were

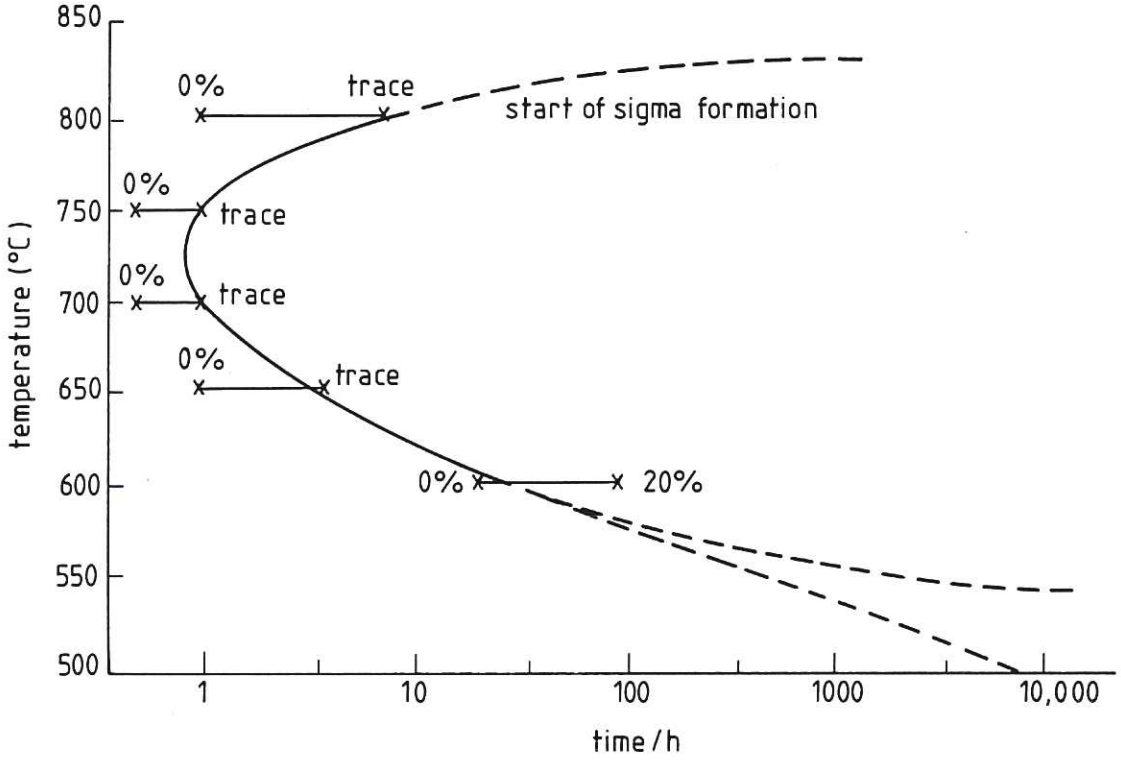

Fig. 6 Diagram illustrating sigma phase transformation kinetics.

CLMR255

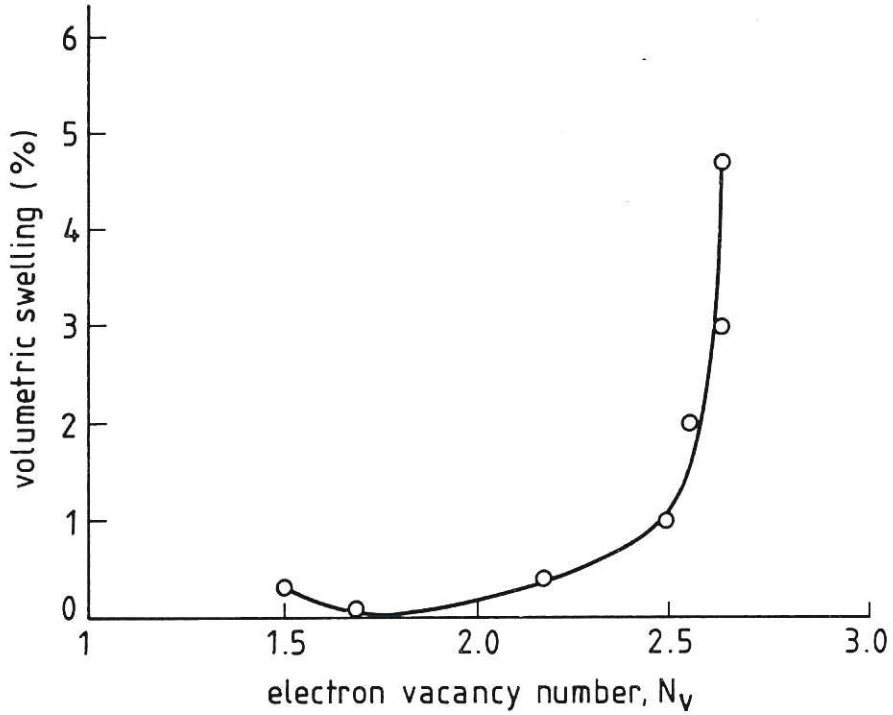

Fig. 7 Observed dependence of radiation-induced void swelling on the electron vacancy number of austenitic stainless steels. The materials were irradiated to 40dpa at 600°–625°C with 46.5MeV Ni^{6-} ions[50].

CLMR255

frequently observed in discrete regions close to MnS particles, implying that swelling might also be reduced in such materials by rigorous control of the sulphur content.

A higher Mn alloy (AMCR) containing 17.5% Mn, 0.057% N, 10% Cr and 0.67% Ni was investigated after irradiation in the HVEM with doses up to 40 dpa at temperatures from 400-650^{0}C[107]. In this case the total swelling was found to increase almost linearly with increasing irradiation dose for temperatures up to 500^{0}C, in helium-free solution-annealed material, reaching about 5% at 40 dpa. For high temperatures the swelling rate increased with dose, a phenomenon that was attributed to a phase instability caused by thin foil effects. This study also concluded that the replacement of nickel by manganese had no adverse effect on the void swelling behaviour of an AMCR-type steel as compared with FV548 and AISI 316 grades. In fact the swelling without helium was observed to be 20-50% lower than that of an AISI 316 steel[21,107]. The peak-swelling temperature was found to be above 650^{0}C, as is the case for Ni-Cr stainless steels.

None of the alloys in the above studies corresponds exactly to the proposed low-activity compositions, which place a higher emphasis on a combination of Mn and N for austenite stabilisation rather than on a combination of Mn, Ni, Cu and/or N. The results available, however, imply a void swelling resistance at least equal to that of the conventional alloys.

8.1.4 Fabrication and mechanical properties of the replacement alloys

When considering the fabricability of the low-activity alloys it is necessary to take into account their potential for transformation into martensite during deformation. The propensity for martensite formation can be related to composition through an equation of the following type[6]:

$$Md_{30}^{50}\ (^0C) = 497 - 462(C+N) - 9.2(Si) - 8.1(Mn) - 13.7(Cr) - 20(Ni) - 18.5(Mo)$$

where Md_y^x is the temperature at which x% of martensite is caused to form by a strain of y; eg. Md_{30}^{50} refers to the temperature at which 50% occurs under a strain of 0.30. The quantification of Md_{30}^{start} is less well established and

some controversy exists regarding the relationship between Md^{x} and Md^{start} (where $0\% < x < 100\%$) with values ranging, for example, from $350^{0}C$ to less than $80^{0}C$[53,93] for $Md_{45}^{start} - Md_{45}^{10}$. In view of this uncertainty, a value of $140^{0}C$ has been assumed for $Md^{start} - Md^{finish}$, in line with that applied for $M_s - M_f$, such that Md_{30}^{start} would be approximately $70^{0}C$ above Md_{30}^{50}. Values of the latter two parameters calculated for all the alloys using the above approach are presented in Table 6 and compared graphically in Fig.8. According to these predicted values the proposed replacement alloys would show a susceptibility to deformation-induced martensite transformation at room temperature comparable to that exhibited by the alloys AISI 321 and FV548. Experimental studies of such steels[94] have revealed a 'bulk' martensite content of some 3% by volume, as determined by magnetic measurements after 20% cold work but a 'surface' value from x-ray analysis and Mössbauer spectroscopy of between 14% and 37% by volume. It was therefore concluded that the α' content could arise from inhomogeneity of the cold rolling deformation or from a lack of constraint and thus greater deformation in the grains at the free surface. Moreover, it was conceded that the α' structure observed by electron microscopy might have been induced during thin foil preparation, thus representing a surface rather than a bulk α' response of the 321 alloy.

The ferromagnetic α' martensite is not the only martensitic phase observed following deformation in Fe-Ni-Cr alloys and austenitic steels; the non-magnetic ε martensite is also frequently present. Whereas the latter predominates in alloys with low stacking fault energies (below 50 mJm^{-2}) only α' is formed in alloys with high stacking fault energies[94]. Some calculations were made to estimate the stacking fault energies for the low activity alloys. Of the predictive equations presented in the literature, that of Schramm and Reed[100] was chosen on account of the attention it pays to the effect of manganese. Though the results cannot be taken as giving absolute values of the SFE it is considered that they should provide a basis for comparison between the alloys. This approach does in fact predict the experimentally observed feature that, of the conventional alloys considered, the 321 steel possesses the lowest stacking fault energy and hence the greatest tendency to form ε martensite. In order to rationalise the calculated values for graphical representation, as in Fig.9, the results are expressed as ΔSFE values, that is to say the value of the SFE calculated for

Table 6 Susceptibility to deformation-induced martensite formation

Alloy	Md_{30}^{50} (°C)		Md_{30}^{start} (°C)	
	max	min	max	min
316	+41	-111	+111	-41
320	+41	-124	+111	-54
321	+84	-29	+154	+41
FV548	+79	-30	+149	+40
HNA2	+132	+33	+202	+103
316T	+104	-20	+174	+51
320T	+104	-33	+174	+37
321T	+107	0	+177	+70
FV548T	+88	+32	+158	+102

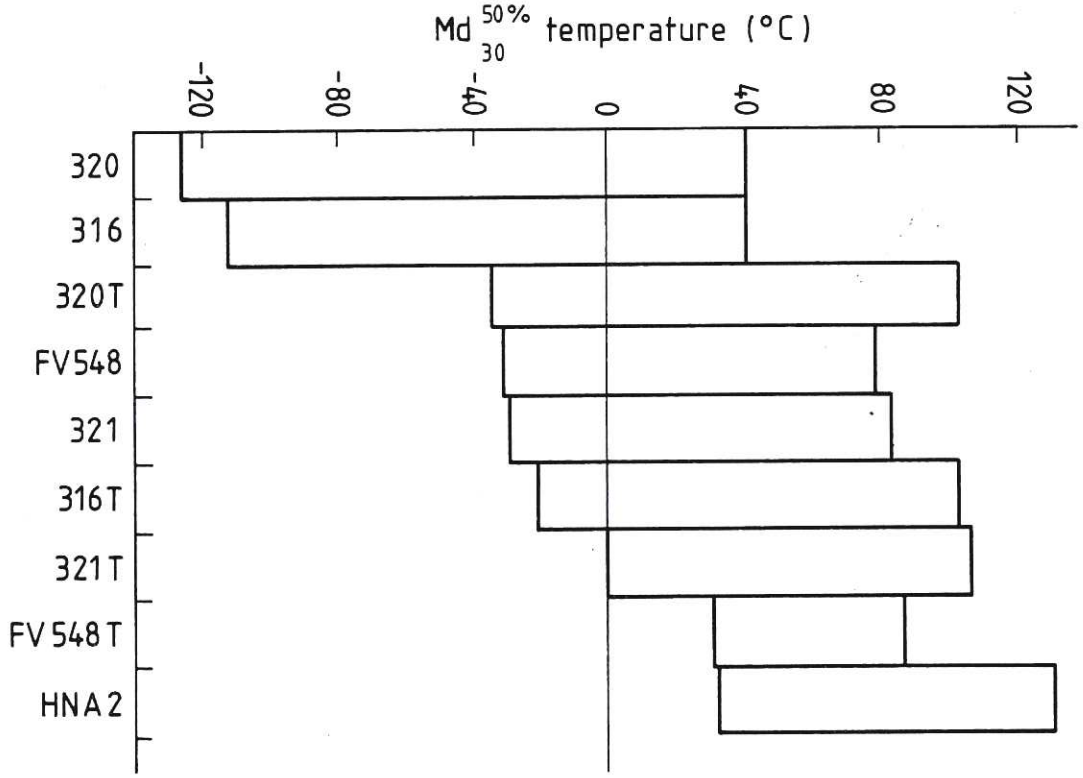

Fig. 8 Chart showing the susceptibility to deformation-induced martensite transformation. The ranges indicated correspond to the composition limits given in Table 2.

CLMR255

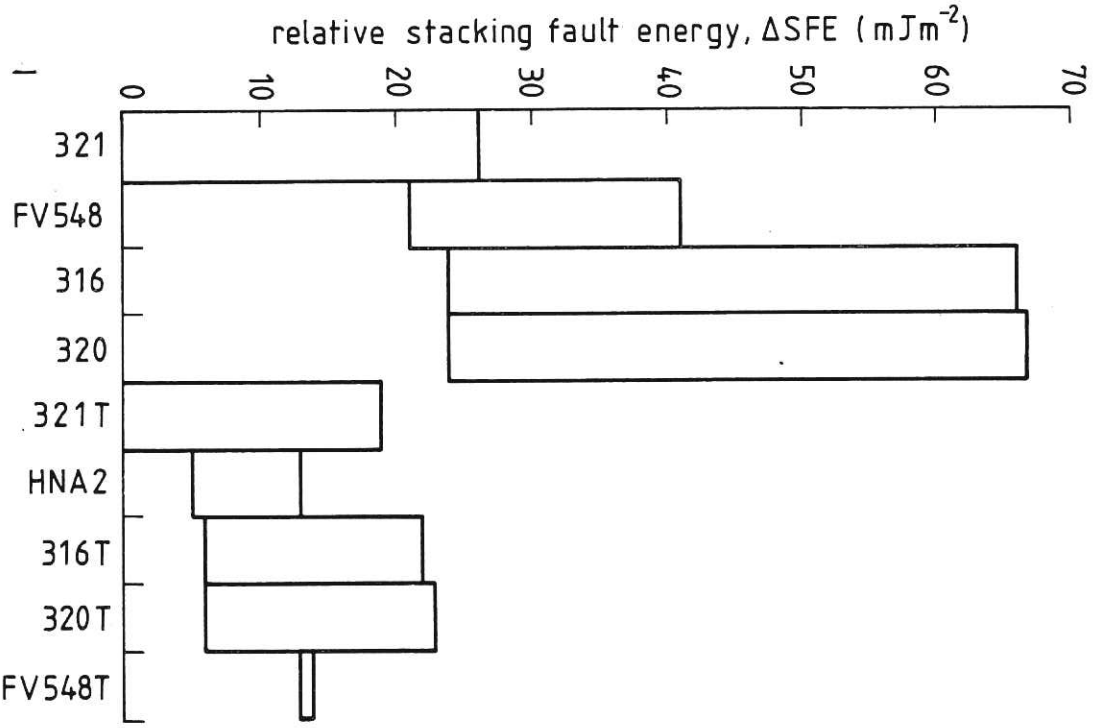

Fig. 9 Chart showing the relative stacking fault energies. Values for the conventional alloys are measured with respect to that for 321 and those for the tailored alloys with respect to that for 321T. The reference values are those corresponding to the lower specification limits and the ranges indicated correspond to the normal composition limits.

CLMR255

the lowest composition limit of the particular alloy and measured relative to the SFE values for the lowest composition limits of those alloys having the smallest SFE, namely alloy 321 in the conventional grades and 321T in the tailored alloys. The quantities obtained by the above method are given in Table 7.

The SFE will tend to influence the mechanical properties and thereby the formability of austenitic steels by two main mechanisms:

(1) The less direct influence is the effect of SFE on the susceptibility to martensite formation during straining. Much controversy has surrounded the austenite → martensite transformation sequence. Recent work on a 321 alloy[94] strongly supports the view that in austenitic steels[110-118] the sequence is $\gamma \rightarrow \varepsilon \rightarrow \alpha'$. If this is the case then the SFE will influence both the amount and type of martensite formed, lower SFE values favouring an enhanced ε martensite formation[110]. In this study on 321 steel it was found that the ε martensite content increased to 20% by volume at about 20% strain during deformation both in tension and during rolling at ambient temperature. The ε content then decreased to zero on increasing the strain from 20% to 50%, while the α' martensite content increased rapidly from below 3% to around 20% by volume during the same strain interval.

(2) A more direct effect is the influence of SFE on the work hardening rate, a reduction of the SFE causing an increase in this rate[95]. The maximum uniform elongation, ε^*, in a tensile test is defined as the strain at which the flow stress and the work hardening rate are numerically equal[46]. A high value of ε^* is beneficial for good stretch forming properties. Thus increasing the work hardening rate relative to the flow stress will increase the maximum uniform elongation, thereby improving the potential for fabrication by stretch-forming techniques. The work hardening rate increases rapidly, however, as martensite is generated and itself participates in the deformation process[46]. Thus increased formation of α' martensite at intermediate strains of 20-50% can lead to maximum uniform elongations considerably greater than those for a stable steel, on account of the resulting higher work hardening rate.

Table 7 Calculated values of the stacking fault energy relative to the stacking fault energy for alloy 321 or 321T (lowest composition limits)

Alloy	SFE (mJm^{-2})
316	24-66
320	24-67
321	0-26
FV548	21-41
HNA2	5-13
316T	6-22
320T	6-23
321T	0-19
FV548T	13-14

Figure 10 shows the effect of Ni content on the maximum uniform elongation and strain at fracture (ε^T) of a 17% Cr steel[46,102]. The curves indicate an optimum concentration of austenite-stabilising element (Ni and, by implication, a Ni-equivalent, referred to the Md^{start} temperature) sufficient to depress the M_s and M_d temperatures such that α' forms only during straining, but insufficient to render the austenitic phase completely stable. According to the calculations of M_s and Md^{start}, such could well be the case for the replacement alloys which, by reference to Fig.10, would probably exhibit values of $\varepsilon^* \sim 0.3$-0.6 and $\varepsilon^T \sim 1.2$-1.6 (true strain).

Predicted values of the 0.2% proof stress and tensile strength for the replacement alloys and the conventional steels are given in Table 8 and compared graphically in Figs.11 and 12. The values were obtained from the following predictive equations[46]:

$$\text{0.2\% Proof stress (MPa)} = 15.4\,[4.4 + 23(C) + 1.3(Si) + 0.24(Cr) + 0.94(Mo) + 1.2(V) + 0.29(W) + 1.7(Ti) + 0.82(A\ell) + 32(N) + 0.46d^{-\frac{1}{2}}]$$

$$\text{Tensile strength (MPa)} = 15.4[29 + 35(C) + 55(N) + 2.4(Si) + 0.11(Ni) + 1.2(Mo) + 5.0(Nb) + 3.0(Ti) + 1.2(A\ell) + 0.82d^{-\frac{1}{2}}]$$

The parameter d in these equations represents the mean grain diameter and was assigned a value corresponding to a typical grain size of ASTM 5. Since the above relationships fail to include the effect of solid solution strengthening by manganese the comparison between the conventional and replacement alloys is not exact but serves only as a general indication. Despite this omission the predicted proof and tensile strength values are higher for the tailored alloys than for the conventional ones and at the high Mn levels proposed there may be some further strengthening from the manganese component.

8.1.5 Creep properties

A detailed knowledge of the creep behaviour of thin-walled components under conditions of elevated temperature, internal-external pressure differences and irradiation is an essential requirement in assessing the performance and

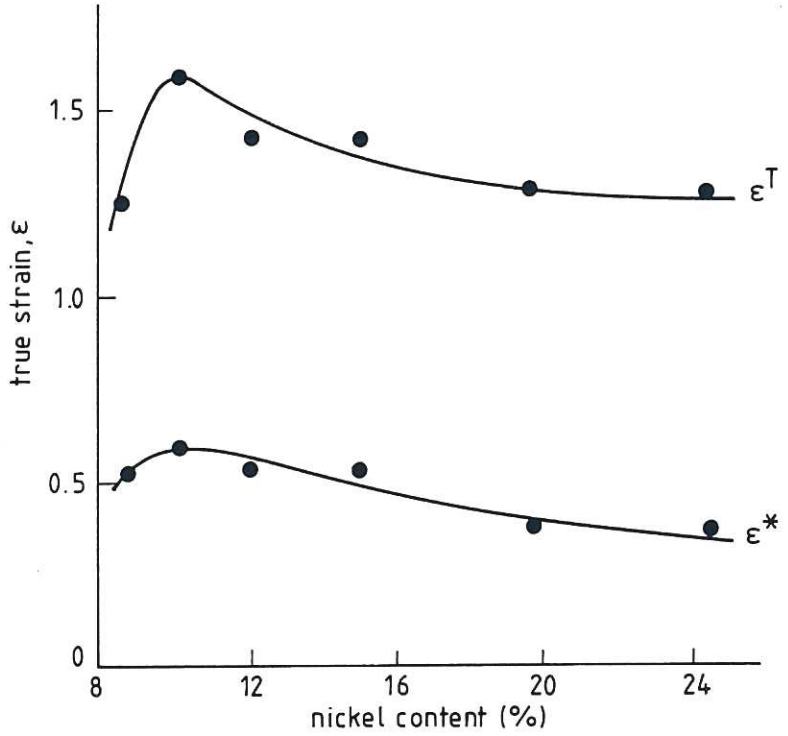

Fig. 10 Graph showing the effect of nickel content on the total ductility, ϵ^T, and the maximum uniform strain prior to plastic instability, ϵ^*, for 17% Cr stainless steel[46].

CLMR255

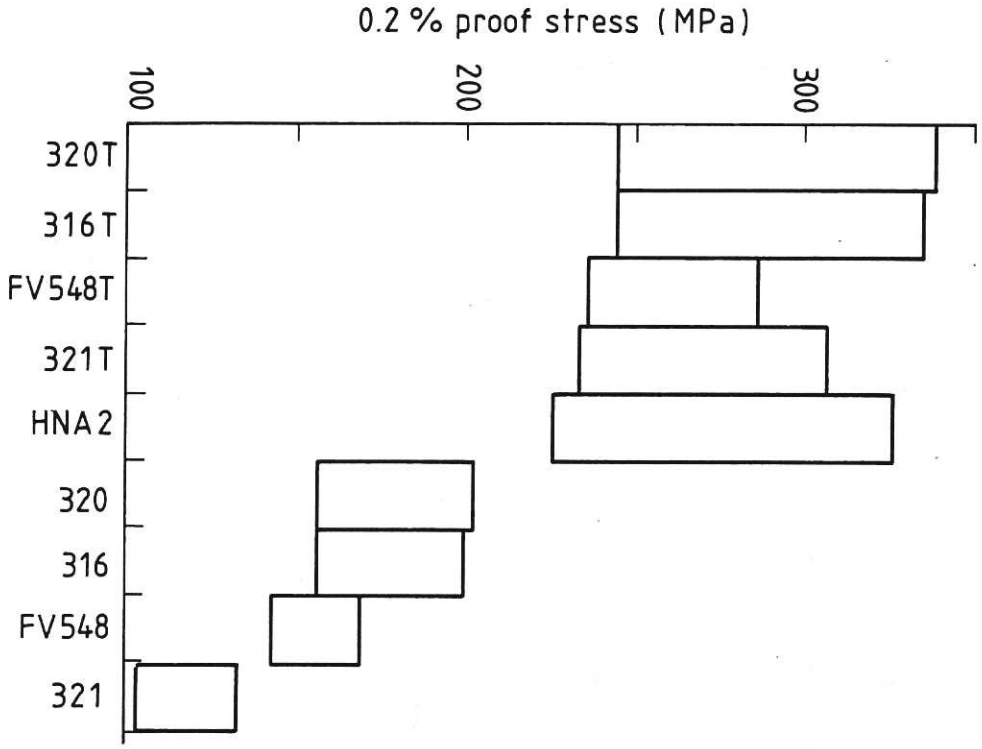

Fig. 11 Predicted values of 0.2% proof stress for the alloys. The ranges indicated correspond to the composition limits listed in Table 2.

CLMR255

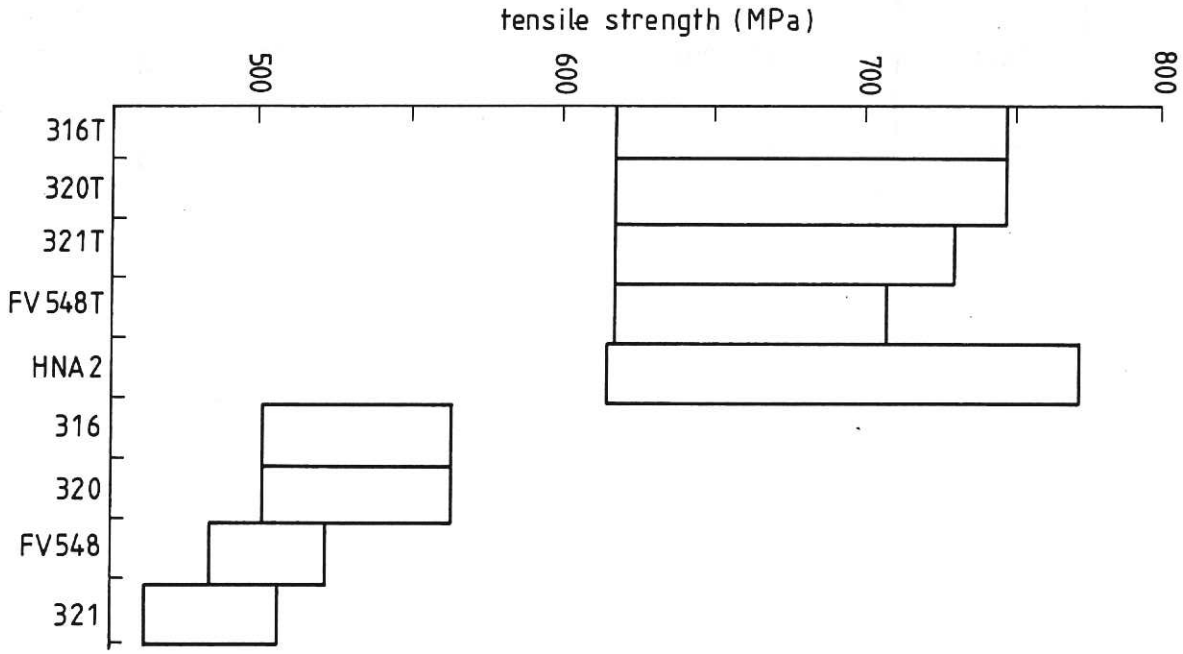

Fig. 12 Chart showing the tensile strengths predicted for the alloys. The ranges correspond to the usual composition limits.

CLMR255

Table 8 Predicted proof stress and tensile strengths

Alloy	0.2% proof stress MPa	tensile strength MPa
316	156-198	501-563
320	156-201	501-563
321	102-132	462-506
FV548	142-168	484-522
HNA2	225-326	616-772
316T	244-334	617-747
320T	244-338	617-747
321T	233-306	617-707
FV548T	235-285	617-707

safety of any reactor system. Whilst much work has been undertaken on the creep properties of austenitic stainless steels there appears to be little published information that would provide the basis for calculation of the rupture lives of the alloys under consideration. Even where empirical relationships have been derived attention has largely been focussed on the effect of carbides precipitated during the creep process, whereas in the tailored alloys it is envisaged that all potential carbide and carbonitride precipitation will have occurred prior to service.

To provide some basis of comparison the following relationship, that allows some account to be taken of 'undissolved' carbides, has been employed[51]:

$$\log_e \text{ rupture life} = (2.4 \pm 2.7) + (7.7 \pm 2.2)(\text{NbCppt}) + (1.24 \pm 0.47)(\text{NbC}_u)$$

where (NbCppt) = NbC available for precipitation during creep period

(NbC_u) = NbC precipitated prior to creep, ie. 'undissolved'.

Although this equation was originally developed for 18% Cr, 13% Ni steels stabilised with Nb, it is considered reasonable in view of the similarities between TaC and NbC to extend its application to alloys stabilised with Ta.

Even with the wide error margins indicated, the above procedure would predict rupture lives of up to only a few hundred hours at about 700^0C and under a stress of 185 MPa for all the present alloys, both conventional and low-activity, if the required conditions of precipitation prior to service are met. The predicted life appears very short and signifies the limited applicability of the relationship to alloys in the fully prior aged condition. It must also be borne in mind that the form in which the 'undissolved' carbides are present would critically affect the degree of creep resistance offered by these alloys. Were these precipitates to be present as relatively few but large particles, rather than as a homogeneous distribution of finer particles, the creep resistance would be appreciably diminished.

8.1.6 Magnetic properties

Since the design and the operation of fusion reactors based on magnetic confinement of the plasma must, at least to some extent, be rendered more complicated if ferromagnetic materials are employed for major components, the absence of ferromagnetism in the austenitic stainless steels confers on them some advantage as first wall and blanket materials. Any phase instability leading to the formation of ferromagnetic products may therefore negate this advantage. Whilst the established austenitic steels do not normally exhibit or develop ferromagnetism under purely thermal conditions, it has been reported that slight ferromagnetism can be detected after irradiation[8]. It has been suggested that an ordered $Ni_3(Fe,Mn)$ phase precipitates under irradiation and may be at least partially responsible for this phenomenon[108]. The proposed low-activity alloys should be superior to the conventional steels in this respect since there is no potential for precipitation of the Ni-rich phase.

The high Mn alloys may, on the other hand, be susceptible to surface-layer instability with respect to α' formation as a consequence of the loss of manganese by evaporation. Moreover, any deformation-induced α' martensite produced during fabrication could also be detrimental in conferring a degree of ferromagnetism on the material. If the Md temperatures predicted for the replacement alloys were to be proved correct then the feasibility of heat treating components prior to service to ensure $\alpha' \rightarrow \gamma$ reversion could be considered, as this would minimise the ferromagnetic permeability and, in particular, prevent local ferromagnetic heterogeneities.

Data in a form that would allow prediction of the magnetic permeabilities of the alloys under study are not readily available in the literature. An attempt has therefore been made to relate the permeability to the alloy composition via the austenite stability, as indicated by the predicted values of M_s and Md_{30}^{50} for the alloys. The permeability values given in Table 9 were obtained from manufacturers' specifications[119]. There was found to be a more distinct correlation of the magnetic permeability with the likely austenite stability, as measured by M_s, than with the parameter Md_{30}^{50}. The trend is illustrated in Fig.13, in which the M_s values are those applicable to a mid-range composition. It appears that the permeability increases with

Table 9 Value of M_s, Md_{30}^{50} and magnetic permeability for the standard grades 316, 321 and 347

Alloy	M_s ^0C	Md_{30}^{50} ^0C	Relative permeability at magnetising field H (kAm^{-1})		
			H = 7.96	H = 39.8	H = 79.6
316	-190	-35	1.008	1.006	1.005
321	-42	+28	2.178	1.641	1.006
347	-57	+74	1.009	1.007	1.006

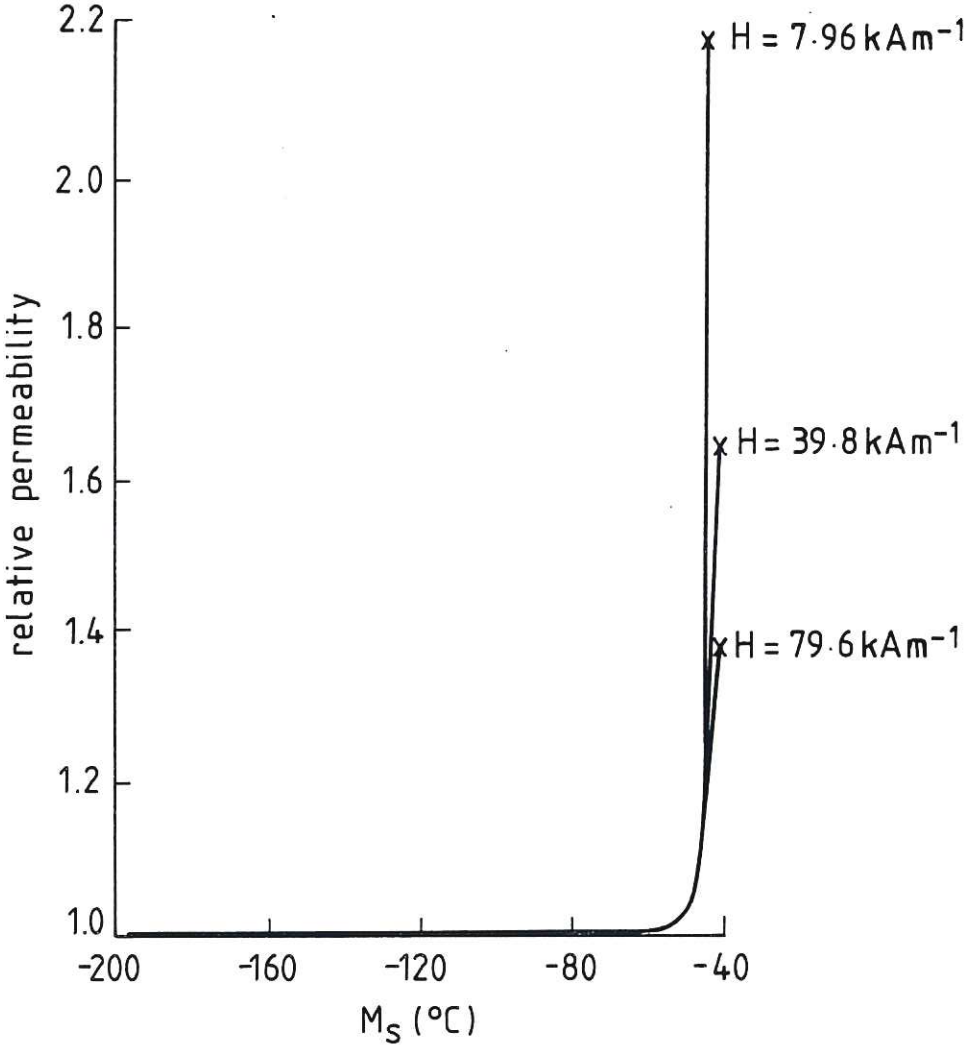

Fig. 13 Variation of the magnetic permeability with M_S temperature.

CLMR255

M_s and Md_{30}^{50} and such a correlation might have been expected as a result of some martensite being induced by specimen preparation for magnetic testing. The calculations show the M_s temperature range, corresponding to the upper and lower limits of the compositional ranges, to be higher for type 321 steel than for the other alloys studied. Reference to Fig.13 would thus suggest relative permeabilities of about 1.2 for all the other conventional grades and replacement alloys. These values could, of course, be expected to increase somewhat with the formation of any strain-induced α' martensite in alloys that proved to be unstable under deformation.

9. CONCLUSIONS

A study based on published information has been performed in an attempt to identify alternative compositions to the current standard 316, 320, 321 and FV548 austenitic stainless steels in order that they may be used as low-activation materials for first wall and breeding blanket components in future fusion reactors. The alternative alloys are required to exhibit a relatively rapid decay of post-irradiation induced activity, such that the surface dose rate from a large slab of the material does not exceed 2.5×10^{-5} Gyh^{-1} after a decay period of 100 years, to facilitate the handling and recycling of expired components. The following conclusions have been drawn from the study.

(1) All the alternative alloys, the compositions of which are given in Table 2b, would meet the required criterion for decay of the dose rate.

(2) The proposed alternative alloys would be expected to possess a fully austenitic structure in the 1050^0C solution treated condition.

(3) The study indicates that there may be some tendency in the alternative alloys to form ε or α' martensite consequent on any cold forming that might be necessary in fabricating the material into components.

(4) It is suggested that the proposed alloys may form sigma-type phases. Because of the low rate of formation of these phases from fully austenitic structures, however, the volume fraction that develops over

the relatively short service life foreseen for steel first wall components may well be acceptable. The tendency toward sigma phase formation under neutron irradiation cannot be evaluated at present and would require experimental investigation.

(5) On the basis of a comparison between the alternative alloys and a similar alloy for which void swelling data are available, it is likely that the proposed alloys would show a significantly higher resistance to void swelling than would conventional 316 steel.

(6) Largely on account of their high nitrogen content the proposed alloys should exhibit up to three times the proof stress of standard austenitic stainless steels.

(7) The formability of austenitic stainless steels, including their weldability, is generally recognised as being superior to that of ferritic stainless steels, which also are candidate first wall and blanket materials. Owing to their somewhat greater propensity to form deformation-induced martensite, the low-activity compositions would be expected to exhibit better formability, especially stretch formability, than the steels they are designed to replace. The increased proof stress may offset this benefit.

(8) Prediction of the creep and rupture properties of the alternative alloys rests on less firm foundations, owing to the lack of data from which confident extrapolation can be made.

(9) Some consideration has been given to the possibility of manganese loss from components during service. Whilst it is possible that such a loss could destabilise the surface layers with respect to ferrite and martensite formation, the rapidity or extent of the phenomenon cannot at present be predicted.

(10) Susceptibility to thermal fatigue has not been considered specifically but, in terms of the thermal conductivity and expansion coefficient, it may be tentatively concluded that the replacement alloys would not be appreciably different from conventional austenitic steels in this respect.

(11) It is possible that, because of their high nitrogen content, the suggested low-activity alloys might suffer from a reduced resistance to lithium attack when used for blanket components in contact with liquid lithium or lithium-lead alloy. This aspect would need to be investigated by experiment.

The general similarity of the proposed alternative alloys to conventional alloys, coupled with their anticipated improved strength and forming characteristics may well allow them to be used for reactor components without excessive expenditure of effort on the development of new production and fabrication technologies.

REFERENCES

1. G.L. Kulcinski, Plasma Physics & Controlled Thermonuclear Research Vol.II, IAEA, Vienna, 1974, p251.

2. B. Badger et al., UWMAK-III, A noncircular power reactor, Univ. of Wisconsin Report 150, 1976.

3. G.L. Kulcinski, Fusion Reactor Design Concepts, IAEA, Vienna, 1978, p573.

4. G.L. Kulcinski, Tokamak Reactors for Breakeven, ed. H. Knoepfel, Pergamon Press, Oxford, 1978, p449.

5. G.L. Kulcinski, Fusion reactors: Their challenge to materials scientists, Contemp. Phys. 20 (1979) 417.

6. B. Badger et al, A Wisconsin tokamak reactor design, UWMAK I, Univ. of Wisconsin Report UWFDM68, 1973.

7. A.P. Fraas, Conceptual design of the blanket and shield region and related systems for a full scale toroidal fusion reactor, ORNL-TM-3096, Oak Ridge National Laboratory, 1973.

8. W.G. Price, Blanket neutronic studies for a fusion power reactor, Trans. Am. Nuc. Soc. 17 (1973) 35.

9. J.D. Lee, Geometry and heterogeneous effects on the neutronics performances of a Yin-Yang mirror reactor blanket, UCRL-75141, Lawrence Livermore Laboratory, 1973.

10. J.R. Powell et al., Studies of fusion reactor blankets with minimum radioactive inventory and with tritium breeding in solid lithium Compounds, BNL-18236, Brookhaven National Laboratory, 1973.

11. D. Steiner, The nuclear performance of vanadium as a structural material in fusion reactor blankets, ORNL-TM-4353, Oak Ridge National Laboratory, 1973.

12. M.A. Abdou and R.W. Conn, A comparative study of several fusion reactor blanket designs, Nuc. Sci. Eng. 55 (1974) 256.

13. R.W. Conn et al., Comparative study of radioactivity and afterheat in several fusion reactor blanket designs, Nuc. Tech. 26 (1975) 391.

14. R.E. Nygren, Materials applications for magnetic fusion, Proc. I.E.E.E. 69 (1981) 213.

15. D.M. Mattox, Coatings for fusion reactor environments, Thin Solid Films 63 (1979) 213.

16. D.M. Mattox and M.J. Davis, Advanced materials for in-vessel components, J.Nuc.Mater. 111 and 112 (1982) 819.

17. D.M. Mattox et al., Thermal shock and fatigue resistant coatings for Magnetically-confined fusion environments, Thin Solid Films 73 (1980) 101.

18. V. Coen et al., Compatibility in Li containing traces of LiH of low-Ni Cr-Mn austenitic stainless steels, J. Nucl. Mater. 85 and 86 (1979) 271.

19. V. Coen et al., Proc. 7th Symposium on Engineering Problems of Fusion Research, Knoxville, Oct. 25-28, 1977, p1501.

20. P. Fenici et al., Influence of lithium exposure on the uniaxial tensile properties of a Cr-Mn austenitic stainless steel, J. Nucl. Mater. 103 and 104 (1981) 699.

21. E. Ruedl et al., Proc. Conf. On Material Behaviour and Physical Chemistry in Liquid Metal Systems, Karlsruhe, March 24-26, 1981.

22. P. Schiller, Material problems in the International Tokamak Reactor, Proc. 3rd ASTM/Euratom Symposium on Reactor Dosimetry, Ispra, 1-5 Oct. 1979, p297.

23. R.E. Nygren, Materials issues in the Fusion Engineering Device, J. Nucl. Mater. 103 and 104 (1981) 31.

24. P.R. Hasiguti, The Japanese Program of Materials Research for Fusion Reactors, ibid.

25. J. Nihoul, The European Programme on Fusion Materials, ibid.

26. P. Schiller, On Materials Problems of the First Wall in INTOR, ibid.

27. A.P. Fraas and H. Postma, Preliminary appraisal of the hazard problems of a D-T fusion reactor power plant, Oak Ridge National Lab. Report ORNL TM.2822, 1970.

28. D. Steiner and A.P. Fraas, Preliminary observations on the radiological implications of fusion power, Nucl. Safety 13 (1972) 353.

29. W.F. Vogelsang, Radioactivity and associated problems in thermonuclear reactors, Proc. Conf. on Technology of Controlled Nuclear Fusion, U.S. Energy R & D Admin., Sept. 1976, Vol.IV, 1303.

30. R.W. Conn et al., Minimizing radioactivity and other features of elemental and isotopic tailoring of materials for fusion reactors, Nucl. Technology 41 (1978) 389.

31. M.S. Kazimi and R.W. Sawdye, Radiological aspects of fusion reactor safety: Risk constraints in severe accidents, J. of Fusion Energy 1 (1981) 87.

32. J.P. Holdren, Contribution of activation products to a fusion accident risk, Part 1, Nucl. Technology/Fusion 1 (1981) 79.

33. J. Crocker and D.F. Holland, Safety and environmental issues of fusion reactors, Proc. I.E.E.E. 69 (1981) 968.

34. O.N. Jarvis, Selection of low activity elements for inclusion in structural materials for fusion reactors, Harwell Report AERE-10426, 1982.

35. J.A. Blink, Neutron activation of four ferritic steels, Lawrence Livermore Lab. Report UCID-19823, 1983.

36. O.N. Jarvis, Low activity materials: Reuse and disposal, Harwell Report AERE-10860, July 1983.

37. R.C. Maninger and D.W. Dorn, Issues in radioactive waste management for fusion power, I.E.E.E. Trans. On Nucl. Sci. 30 (1983) 571.

38. E.C. Bain and W.E. Griffiths, An introduction to the iron-chrome-nickel alloys, Trans. AIME 75 (1927) 166.

39. G.V. Raynor et al., Phase equilibria in iron ternary alloys. I- A critical evaluation of the constitution of the Cr-Fe-Ni system, Int. Met. Revs. 25 (1980) 21.

40. A.J. Bradley et al., An X-ray investigation of iron-nickel-chromium alloys, J.I.S.I. 2 (1941) 273.

41. W.P. Rees et al., Constitution of iron-nickel-chromium alloys at 650° to 800°C, J.I.S.I. 1949, July, 325.

42. A.J. Cook et al., The constitution of Fe-Ni-Cr alloys, ibid, 171.

43. B. Hattersley et al., Constitution of certain austenitic steels, J.I.S.I. 204 (1966) 683.

44. L. Kaufman et al., Computer Calculations of Phase Diagrams, Academic Press, New York, 1970.

45. C. Zapfe, Stainless Steels, A.S.M. 1949.

46. F.B. Pickering, Physical Metallurgy and the Design of Steels, Applied Science Publishers, 1978.

47. L. Pryce and K.W. Andrews, Practical estimation of composition balance and ferrite content in stainless steels, J.I.S.I. 195 (1960) 415.

48. J.Z. Briggs and T.D. Parker, The Super 12% Cr Steels, Climax Molybdenum Co., 1965.

49. H. Schneider, Investment casting of high-hot-strength 12% chrome steel, Foundry Trade Journal 108 (1960) 562.

50. D.R. Harries, Physical metallurgy of Fe-Ni-Cr austenitic stainless steels, Int. Conf. on Mechanical Behaviour and Nuclear Applications of Stainless Steels at Elevated Temperatures, Varese, 20-22 May, 1981.

51. S.R. Keown and F.B. Pickering, Creep Strength in steel and high temperature alloys, Proc.Conf. 20-22 Sept. 1972, Sheffield, Publ. Met. Soc. 134.

52. M. Deighton, Solubility of NbC in 20%Cr-25%Ni stainless steel, J.I.S.I. 205 (1967) 535.

53. K.W. Andrews and H. Hughes, Proc. Conf. on Precipitation Processes in Steels, Sheffield I.S.I. Spec.Rep. No. 64 (1958) 124.

54. A.H. Bott, PhD Thesis, Sheffield City Polytechnic, 1984.

55. K.J. Irvine et al., High strength austenitic stainless steels, J.I.S.I. 199 (1961) 153.

56. E.J. Dulis, Age-hardening austenitic stainless steels, I.S.I. Spec. Rep. No. 86 (1964) 162.

57. C.M. Hsiao and E.J. Dulis, Phase relationship in austenitic Cr-Mn-C-N steels, Trans. A.S.M. 50 (1958) 773.

58. C.M. Hsiao and E.J. Dulis, Precipitation reactions in Cr-Mn-C-N steels, ibid. 49 (1957) 655.

59. G.J. Eichelman and F.C. Hull, Effects of composition on the temperature of spontaneous transformation of austenite to martensite in 18-8 type stainless steel, ibid. 45 (1953) 77.

60. F.C. Monkman et al., Computation of M_s for stainless steels, Met. Prog. 71 (1957), 94.

61. T. Angle, Formation of martensite in austenitic stainless steels. Effects of deformation, temperature and composition, J.I.S.I. 173 (1954) 165.

62. R.F. Decker et al., Trends In high temperature alloys, Am.Inst.Min.Met., Pet.Eng.Conf.Proc. 28 (1965) 69.

63. F.R. Beckitt, The formation of sigma-phase from delta ferrite in a stainless steel, J.I.S.I. 207 (1969) 632.

64. L. Columbier, Mo in Stainless Steels and Alloys, Climax Molybdenum Co.Ltd., 1968.

65. H. Wiegand and M. Doruk, Effect of carbon and molybdenum on precipitation processes, Arch. f.d. Eisen. 33 (1962) 559.

66. H.J. Goldschmidt, The structure of carbides in alloy steel, J.I.S.I. 163 (1949) 381.

67. E.T. Dulis and G.V. Smith, Identification and mode of formation and resolution of sigma phase in austenitic Cr-Ni steels, A.S.T.M., S.T.P., 110(1950) 1.

68. R.E. Lismer et al., A microscopical examination of iron containing manganese inclusions, J.I.S.I. 171 (1952) 48.

69. F.B. Pickering, The formation of sigma phase in austenitic stainless steel, I.S.I. Spec.Rep. No. 64 (1959) 118.

70. P.A. Blenkinsop and J. Nutting, Precipitation of the sigma phase in an austenitic stainless steel, J.I.S.I., 1967 Sept., 953.

71. L. Pauling, Nature of interatomic forces in metals, Phys. Rev. 54 (1938) 899.

72. S.P. Rideout et al., Intermediate phases in ternary alloy systems of transition elements, J. of Met. 3 (1951) 872.

73. A.J. Sully et al., J. of Heat Treatment 1 (1948) 228.

74. P. Greenfield et al., The sigma phase in binary alloys, Trans. A.I.M.E. 200 (1954) 253.

75. P. Greenfield et al., Intermediate phases in binary systems of certain transition elements, ibid. 206 (1956) 265.

76. W.J. Boesch et al., Preventing sigma phase embrittlement in nickel-base superalloys, Met. Prog. 86 (1964) 109.

77. L.R. Woodyatt et al., Prediction of sigma-type phase occurrence from compositions in austenitic superalloys, J.T.M.S. 236 (1966) 519.

78. R.F. Decker, Int. Symp. on Strengthening Mechanisms in Steels, Zurich, Climax Molybdenum Co., 1969, p147.

79. J. Cawley, PhD Thesis, Sheffield City Polytechnic, 1982.

80. G.W. Greenwood et al., Role of vacancies and dislocations in nucleation and growth of gas bubbles in irradiated fissile material, J. Nuc. Mater. 51 (1959) 305.

81. C. Cawthorne et al., The influence of irradiation temperature on the defect structures in stainless steel, A.E.R.E. Report R5269 (1969) p446.

82. C. Cawthorne et al., Voids in irradiated stainless steel, Nature 216 (1967) 575.

83. D.R. Harries, Void swelling in austenitic steels and nickel based alloys: Effects of alloy constitution and structure, A.E.R.E. Report R7934, Jan. 1975, p287.

84. T.M. Williams et al., The void swelling behaviour of solution treated FV 548 stainless steel irradiated with 22 MeV C^{2+} and 46 MeV Ni^{6+} ions and the influence of heat treatment, J. Nucl. Mater. 88 (1977) 69.

85. T.M. Williams et al., Void swelling in cold worked FV548 steel Irradiated in a high voltage electron microscope after pre-irradiation with 10 ppm He, ibid. 64 (1977) 183.

86. T.M. Williams et al., Interstitial loop nucleation and growth in solution treated type 316 stainless steel irradiated to low doses with 22 MeV C^{2+} and 46 MeV Ni^{6+} ions, J. Nucl. Mater. 79 (1979) 28.

87. M.J. Makin, radiation effects in breeder reactor structural materials, Int. Conf. Proc. Scottsdale, Arizona, June 1977.

88. W.G. Johnston et al., Proc. A.S.M. Sci. Seminar, Cincinnati, Nov. 1975, 429.

89. W.G. Johnston et al., An experimental survey of swelling in commercial Fe-Cr-Ni alloys bombarded with 5 MeV Ni ions, J. Nucl. Mater 54 (1974) 24.

90. J.S. Watkin et al., Int. Conf. Proc. Scottsdale, Arizona, June 1977, 84.

91. D. Mosedale et al., Radiation effects in breeder reactor structural materials, ibid, 129.

92. I. Williams et al., Stability of austenitic stainless steels between 4K and 373K, Proc 6th Int. Cryogenic Conf., Grenoble, 1976, 337.

93. D.C. Larbalestier and H.W. King, Prediction of the low-temperature stability of type 304 stainless steel from a room-temperature deformation test, Proc. 4th Int. Cryogenic Conf. 1972, 338.

94. M.W. Bowkett and D.R. Harries, Martensitic transformations in cold rolled EN 58B (Type 321) austenitic stainless steel, A.E.R.E. Report R9093, 1978.

95. J. Nutting, The physical metallurgy of alloy steels, J.I.S.I. 207 (1969) 872.

96. J. Nutting and D. Dulieu, Influence of solute additions on the stacking fault energy of iron-nickel-chromium austenites, I.S.I. Spec. Rep. No.86, 1964, 140.

97. P.R. Swann, Dislocation substructure vs. transgranular stress corrosion susceptibiltiy of single phase alloys, Corrosion 19 (1963) 102.

98. R. Barnatt et al., Stress corrosion cracking mechanism in purified 16%Cr-20%Ni stainless steel, Corrosion Sci. 3 (1963) 9.

99. P.C.J. Gallagher, The influence of alloying, temperature and related effects on the stacking fault energy, Met. Trans. 1 (1970) 2461.

100. R.E. Schramm and R.P Reed, Stacking fault energies of seven commercial austenitic stainless steels, Met. Trans. 6 (1975) 1345.

101. S.W. Yang and J.E Spruiell, Cold worked state and annealing behaviour of austenitic stainless steel, J. Mat. Sci. 17 (1982) 677.

102. K.J. Irvine et al., The strength of austenitic stainless steels, J.I.S.I 207 (1969) 1017.

103. F.B. Pickering, Towards improved ductility and toughness, Climax Molybdenum Symp., 1972, 9.

104. F.B. Pickering, I.S.I. Spec.Rep. No. 84, 1972.

105. T. Gladman et al., Austenitic stainless steels for cold forming, Sheet Metal Industries 51 (1974) 219.

106. H.J. Goldschmidt, Interstitial Alloys, Butterworths, London, 1967.

107. M. Snykers and E. Reudl, Radiation damage simulation experiments on a Mn-Cr austenitic stainless steel in a H.V.E.M., Proc. 11th Symp. on Fusion Technology, Oxford, 15-19 Sept., 1980.

108. C. Brown et al., The occurrence of an ordered F.C.C. phase in neutron irradiated M316 stainless steel, J. Nucl. Mater. 66 (1977) 201.

109. D.J. Mazey et al., Observations of microstructure and void formation in a 8% Mn stainless steel (I.C.L. 016) irradiated with 46 MeV nickel ions, A.E.R.E. Report R9931, 1980.

110. P.M. Kelly, The martensite transformation in steels with low stacking fault energy, Acta. Met. 13 (1965) 635.

111. C.J. Gunter and R.P Reed, Effect of experimental variables including the martensite transformation on the low temperature mechanical properties of austenitic stainless steels, Trans. A.S.M. 55 (1962) 399.

112. B. Cina, Effect of cold work on the $\gamma \rightarrow \alpha$ transformation in some Fe-Ni-Cr alloys, J.I.S.I. Aug 1954, 406.

113. J.A. Venables, The martensite transformation in stainless steel, Phil. Mag. 7 (1962) 35.

114. P.L. Manganon and G. Thomas, The martensite phases in 304 stainless steel, Met. Trans. 1 (1970) 1577.

115. J. Dash and H.M. Otte, The martensite transformation in stainless steel, Acta. Met. 11 (1963) 1169.

116. A.J. Goldman et al., The association of H.C.P. and B.C.C. structures in the martensite transformation, Trans. A.I.M.E. 230 (1964) 195.

117. D.T. Llewellyn and J.D. Murray, Cold worked stainless steels, I.S.I. Spec.Rep.86, 1964, 197.

118. A.N. Vorobyev et al., Radiation effects on mechanical properties and Microstructure of solution-treated and cold-worked 1 X 18H10T and 0 X 16H15M 3B stainless steels, European Conference on Irradiation Behaviour of Fuel Cladding and Core Component Materials, Karlsruhe,Dec.1974.

119. Silver Fox Hi-Proof Stainless Steels, Publ. British Steel Corp., (Alloy Property Specs), Special Steels Division, Stocksbridge Works, Sheffield.

Available from
HER MAJESTY'S STATIONERY OFFICE
49 High Holborn, London, WC1V 6HB
(Personal callers only)
P. O. Box 276, London, SE1 9NH
(Trade orders by post)
13a Castle Street, Edinburgh, EH2 3AR
41 The Hayes, Cardiff, CF1 1JW
Princess Street, Manchester, M60 8AS
Southey House, Wine Street, Bristol, BS1 2BQ
258 Broad Street, Birmingham, B1 2HE
80 Chichester Street, Belfast, BT1 4JY

PRINTED IN ENGLAND